Studies of Surface Chemical Physics Using Nuclear-Spin-Polarized Atomic Beams

R. F. HAGLUND, JR.

Department of Physics and Astronomy and Center for Atomic and Molecular Physics at Surfaces, Vanderbilt University, Nashville, Tennessee 37235

Received February 9, 1988 (Revised Manuscript Received March 30, 1988)

Contents

Richard Haglund is Associate Professor of Physics at Vanderbilt University. He received the B.A. degree from Wesleyan University, and a Ph.D. in experimental nuclear structure physics at the University of North Carolina, Chapel Hill, in 1975. He continued his research in few-nucleon scattering and reactions with polarized deuterons and tritons during a postdoctoral appointment at the Los Alamos National Laboratory. In 1977, Professor Haglund became a staff member in a laser physics group at Los Alamos and participated in the construction and development of high-power infrared and ultraviolet lasers for laser fusion research. After a sabbatical year at the Philipps-Universität in Marburg, West Germany, as an Alexander von Humboldt Fellow—during which his interest in the topic of this review paper began—he served as a group leader for laser physics and applications at Los Alamos prior to going to Vanderbilt in 1984. Professor Haglund's current research interests include desorption induced by electronic transitions, laser–matter interactions, and the use of nuclear-spin-polarized atomic beams as probes of surface structure and dynamics. He is a member of Phi Beta Kappa, the American Physical Society, and the Optical Society of America.

I. Summary

Nuclear magnetic resonance (NMR) measurements have been widely used for many years as analytical tools in condensed-matter physics, chemistry, biology, and medicine. Thus far, the use of NMR in the study of surfaces and interfaces has been relatively less ubiquitous, primarily because of limitations on sample size inherent in surface studies. Recently, however, it has been demonstrated that thermal velocity beams of nuclear-spin-polarized alkali atoms, adsorbed on hot metal surfaces, are sensitive to important details of both surface structure and surface dynamics. The high polarization of the probe beams, when coupled with the efficiency of atomic physics techniques used for monitoring the polarization of desorbed particles, makes possible a variety of interesting spin relaxation experiments on single-crystal surfaces, including a novel kind of nuclear magnetic resonance. Extension of the current experimental techniques to semiconductor and insulator surfaces at arbitrary temperatures appears to be possible, perhaps even straightforward. Thus far, this new technique has been used to probe adsorbate-induced changes in surface field gradients, electronic structure at surfaces, the surface-adsorbate resonance near the Fermi level, and measurements of absolute diffusion rates for atomic adsorbates. Moreover, the variety of presently or potentially available polarized nuclear species suggests that the chemistry of many interesting

0009-2665/88/0788-0697$06.50/0

adsorbate–surface systems, including hydrogen, alkalis, halogens, and rare gases, could be profitably investigated by this method.

II. Introduction

Almost from the moment of its discovery as a fundamental physics phenomenon,[1] the utility of nuclear magnetic resonance spectroscopy as an analytical tool was inescapable. Because of the detailed information it provides about the electromagnetic field distributions in solids, gases, and liquids, NMR, together with electron spin resonance and combined optical–rf resonance techniques, has become a firmly established component of a large and enormously successful branch of atomic and molecular spectroscopy based on spin relaxation diagnostics. Also, because NMR is an essentially noninvasive technique, it has been invaluable in studies of living systems, culminating most recently and stunningly in the development of magnetic resonance imaging technology for medical applications.

However, one significant area of study has been relatively resistant to the applications of NMR techniques: the study of surfaces and interfaces. To a significant degree, this arises, as has often been observed, from problems of sample size and detection efficiency. Conventional NMR measurements are made possible by tiny variations of the nuclear magnetic substrate populations in the Boltzmann distribution induced by a large magnetic field. Because of the small induced polarization, a large sample density of probe nuclei is required in order to yield detectable signals: even with modern techniques of signal processing and pulse sequencing. NMR experiments typically require from 10^{17} to 10^{19} nuclear spins to produce detectable signals. But a surface has only some 10^{14}–10^{15} atomic sites per square centimeter; thus, for example, an NMR study by conventional techniques would necessitate something of order one meter square as a sample surface! In surface chemistry studies related to catalysis,[2,3] this limitation has been overcome by using finely divided particles as samples, which is appropriate, particularly since this is often the physical form in which catalytic materials are used anyway. Even then, however, the interpretation of the experiments is not always unambiguous, because it is generally difficult to distinguish between the bulk and surface signals. Moreover, in that other interesting branch of surface science—the study of physics at single-crystal surfaces—the limitation on sample size is both essential and inescapable. The sophisticated spin perturbation and signal detection schemes employed in NMR studies of surface processes in catalysis simply are not effective in surface *physics*, where many of the model systems of greatest interest are single-crystal surfaces with low adsorbate coverage. It thus appears that it is simply not possible to use conventional magnetic resonance techniques in these circumstances.

Recently, however, experiments using nuclear-spin-polarized atomic beams to probe single-crystal metal surfaces have shown one possible solution of this problem.[4] In the nuclear magnetic resonance studies based on polarized-beam techniques described here, the difficulties endemic to powders or finely divided particles do not arise, because the polarization of the beam is created in a source and because the polarization detection scheme is completely surface specific in that *only* desorbed atoms that have interacted with the surface are detected. Neither low temperatures nor high magnetic fields are required; indeed, the only components of polarized-beam NMR apparatus having anything in common with conventional magnetic resonance hardware are the rf field coils mounted near the sample surface.

Moreover, unlike conventional ion surface scattering or electron diffraction methods, surface spectroscopy with adsorbed spin-polarized nuclei is sensitive directly to details of the surface charge distribution in the neighborhood of the adsorption site, making this a promising technique for the analysis of both surface structure and surface dynamics. The information gleaned thus far suggests that this technique has the potential for helping to accomplish in surface physics what spin resonance and spin relaxation studies have already done in unraveling the mysteries of charge distributions in bulk condensed matter. However, careful examination of the underlying physics of the technique has also raised a host of questions about the detailed dynamics of the adsorption and desorption of the polarized probes, which will have to be dealt with through relevant surface physics studies. Of course, desorption spectroscopy with nuclear-spin-polarized probes is not a philosopher's stone for surface chemical physics, but rather one more tool borrowing useful capabilities from another traditional field of physics—in this case, nuclear structure physics—to be applied to the very complex problems of surface electronic structure and dynamics.

In this review, we present the conceptual elements of the experiments, describe the experimental apparatus, and then consider some of the results of the past few years' studies of polarized lithium and sodium nuclei on hot metal surfaces. We then pass to a consideration of ways to extend current techniques to permit studies of semiconductor and insulator surfaces at arbitrary temperatures and to the potential for work with other probe species—ranging from halogens to odd-nucleon-number ("odd A") noble gases and the hydrogen isotopes. The apparent possibilities for creating beams with a large number of probe species and for applying the technique to other surfaces suggest that surface spin relaxation experiments with polarized beams are likely to yield qualitatively new and significant information about fundamental problems as a surface analytical tool in both chemistry and physics.

III. Nuclear Surface Physics Experiments and Their Interpretation

The essentially serendipitous discovery of the potential for using polarized beams in surface physics arose out of the construction of a spin-polarized ^{6}Li ion source for nuclear physics studies by a group from the University of Hamburg and later by Fick and collaborators.[5,6] In their polarized-ion source, a thermal atomic beam was electron spin polarized by passing through the spatially inhomogeneous field of a multipole magnet and then nuclear spin polarized by an adiabatic transition in combined magnetic and rf fields.[7] The atoms were then prepared for injection into a tandem Van de Graaff accelerator by surface ionization on a heated tungsten ribbon. Following successful experiments with

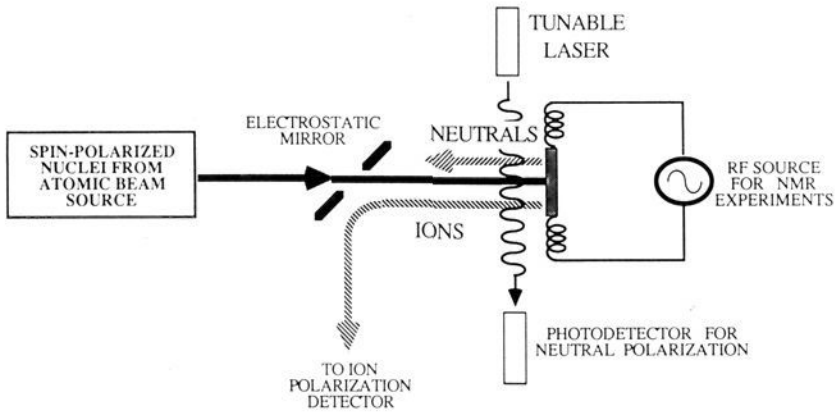

Figure 1. Schematic diagram of a SPNSS experiment, showing major functions and apparatus.

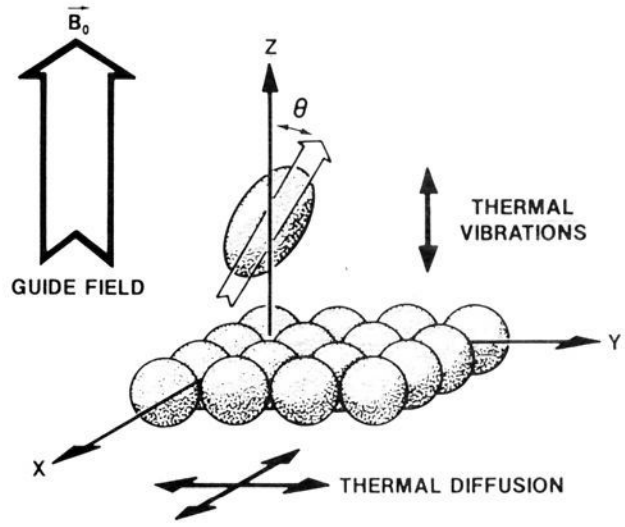

Figure 2. Schematic of a polarized nucleus residing on a surface. The z axis is defined to be in the direction of the magnetic guide field and is usually perpendicular to the surface.

polarized ^{6}Li nuclei, the ion source was reconfigured to produce beams of ^{7}Li, whereupon it was observed[8] that the nuclear polarization was drastically reduced for the ions desorbing from the surface ionizer—a puzzling situation at first glance because of the presumption that the nuclei should not be affected by surface electronic processes. Upon further reflection, however, it became apparent that the ionically bound ^{7}Li atom, once adsorbed on the surface, would effectively have only an inert closed shell of electrons and a nucleus now free to interact with its surroundings during its residence time on the surface ionizer. The larger depolarization rate of ^{7}Li relative to ^{6}Li was attributable to its significantly larger nuclear quadrupole moment (37 mb compared to 0.8 mb for ^{6}Li) and the consequently higher interaction cross section for a given surface ionizer temperature and material. This insight led rapidly to the understanding that beams of polarized nuclei could provide a unique and powerful probe of surface electromagnetic fields in the vicinity of surface sites where they were adsorbed,[4] thus sidestepping some of the difficulties of applying conventional magnetic resonance techniques to surfaces.

The essential features of a generic nuclear surface physics experiment are illustrated in Figure 1. A beam of nuclear-spin-polarized alkali atoms is incident on the sample surface at thermal velocity; a large fraction of these probe nuclei are adsorbed on the surface, where they remain until desorption occurs. During the residence time of the polarized nuclei on the surface, they interact with the surface magnetic fields and electric field gradients or with any applied electromagnetic fields through their magnetic dipole and electric quadrupole moments, respectively. Depending on the relative sizes of the dipole and quadrupole moments, the interaction may be primarily with the magnetic field, primarily with the electric field gradient, or with some combination of the two. After a residence time determined by the experimenter's choice of desorption technique, both polarized atoms and ions desorb, whereupon their polarization is once again measured, either by beam-foil spectroscopy (in the case of desorbing ions) or by laser-induced fluorescence in a magnetic field (for desorbing atoms). The measured change in polarization is related to the surface fields in a manner that we now describe briefly.

The formalism for describing the interactions of the nuclear spins with their surface environment combines features from the analysis of nuclear magnetic resonance in bulk materials[9,10] and from nuclear reaction analysis.[11] The problem is essentially one of describing the polarization state of a nucleus with known nuclear moments M_{kq} interacting with a distribution of charges and (possibly) external fields whose net effect is describable by means of a set of multipole fields V_{kq}. In the coordinate system of Figure 2, the z axis is perpendicular to the surface, while the x and y coordinates are defined to be in the plane of the surface. The quantization axis is defined by the external guide magnetic field, generally, but not always, chosen to be the z axis. Both Cartesian and spherical tensor notations are used to describe operators and fields, depending on what is most natural for describing the physics. It is helpful to remember that the multipole fields $V_{kq}(t)$ and the spin operators M_{kq} have only z components when $q = 0$, and only x or y components for $q \neq 0$.

From the analytical point of view, the description of an ensemble of polarized particles is most easily managed by using density-matrix formalism.[12] The polarization state of an ensemble of nuclei of spin I with possible spin projections m, m', ... can be specified by a density operator or density matrix defined in terms of the familiar bra and ket vectors of quantum mechanics by

$$\rho \equiv |Im\rangle\langle Im'|$$

The diagonal elements of the density matrix ρ_{mm} are just the relative occupation numbers N_m of the nuclear magnetic substates. In order to more fully exploit the physical symmetries of a problem, it is often more convenient to use irreducible tensor operators than the density matrix itself. Here we shall describe the polarization state of an ensemble of nuclei using spherical polarizations tensors (or state multipoles, as they are sometimes called), which have the virtue of transforming in the same way as the multipole fields V_{kq}. These polarization tensors of rank k and order q for a nucleus with total angular momentum I are related to the elements of the corresponding density matrix by the equation

$$t_{kq} = \sqrt{(2I+1)}\sqrt{(2k+1)}\sum_{mm'}(-1)^{I-m-q}(IIk|m-m'q)\rho_{mm'}{}^{I} \quad (1)$$

where the quantity in parentheses is a Wigner 3-J coefficient and where k and q are constrained to the values $|k| \leq 2I$, $|q| = 0, 1, ..., k$ by their relations to the total angular momentum of the nuclei in the ensemble.

State multipoles with $k = 1$ are often called "vector polarizations", because they specify the orientation vector of the system and are proportional to its net magnetic dipole moment; another way of expressing that fact is to note that these state multipoles are proportional to the spherical components of the *first-order* multipole fields, the various components of the magnetic induction **B**. Similarly, the second-rank polarization tensors with $k = 2$ are frequently called "alignment tensors", because they are proportional to the components of the *second-order* multipole fields, that is, to the components of the electric quadrupole tensor.[12]

The t_{kq}, in turn, are related to the Cartesian polarization tensors P_{ijk} through various proportionality constants. The relationships between the elements of the density matrix and the various components of the Cartesian and spherical polarization tensors are given explicitly in the Appendix for particles of spin 1 and spin $^3/_2$.

The mathematical formalism of the density matrix reflects the experimental situation: in thermodynamic terms, we have a system S consisting of the nuclear spins in contact both with an external reservoir R (the surface) and with external applied fields. The interactions of the polarized nuclei both with the reservoir and with the external fields are described by the potentials V_{kq}, so that these potentials will have, in general, both "static" (deterministic) and fluctuating (random) components. The time evolution of the density matrix is dependent both on slowly varying components of the surface or applied fields and on relaxation terms representing the loss of polarization to the unobserved reservoir of surface atoms R. It is expressed by the Liouville equation and is

$$\frac{ih}{2\pi}\frac{\partial\rho}{\partial t} = [\mathcal{H}(t),\rho(t)] \qquad (2)$$

where the equation is understood to refer to the appropriate operators; the same statement can be cast in terms of matrix elements by taking the conventional "sandwich" between bra and ket vectors for the appropriate magnetic substates on both sides of the equation. The Hamiltonian describing the interaction with the surface fields in the vicinity of the probing polarized nucleus is

$$\mathcal{H}(t) = \sum_{k,q}(-1)^q V_{kq}(t)M_{k-q} = V_{00}M_{00} + V_{11}M_{11} + V_{10}M_{10} + V_{1\text{-}1}M_{1\text{-}1} + \ldots \qquad (3)$$

where the M_{kq} are the nuclear multipole operators. Thus the Liouville equation produces the direct connection between the depolarization rate(s), the known multipole moments of the polarized nuclear probes, and the surface multipole fields. Note that the first term in the Hamiltonian involves only the electric charge of the nucleus and has, of course, no effect on the spin. The higher order dipole and quadrupole terms give the interactions that change the polarization; the strength of those terms, including the relative weight of the dipole and quadrupole interactions, is determined by the magnitude of the moments for a given nucleus. The V_{kq} include both the effects of the fluctuating electromagnetic fields of the surface and any applied fields used to perturb the spin. In interpreting the results of any particular experiment, it is necessary to determine the relative strength of these two components; in general, it is in fact advantageous to deal only with one or the other by a careful choice of experimental conditions. Explicit expressions for the multipole moments and the multipole fields are given in the Appendix.

In the quantum theory of relaxation, it is demonstrated that the equation of motion for the density matrix of a spin system S in contact with a dissipative reservoir of states R has the form of a Pauli master equation:

$$\dot{\rho}(t)_{mm} = \sum_{n\neq m}\rho(t)_{nn}W_{mn} - \rho(t)_{mm}\sum_{n\neq m}W_{nm} \qquad (4)$$

where the quantities W_{kl} represent the transition probabilities from one quantum state $|l\rangle$ to another quantum state $|k\rangle$. This equation is a simple statement that the probability of finding the atomic level $|m\rangle$ occupied at some time t increases because of transitions from other occupied states into m and decreases in proportion to the sum over all the possible transition probabilities out of that state. The quantities W_{kl}, in turn, can be related (see Appendix) both to the reversible interactions with the external (surface and applied) fields and to the interactions of the spin system S, with the reservoir states R leading to an irreversible relaxation of the spins in S. The transition probabilities turn out to be

$$W_{mm'} = \sum_{kk'}J_{kk'}(\omega_{mm'})|U^*_{k\text{-}q}|\cdot |U_{k'q}|(IIk|m\text{-}m'q)(IIk'|m\text{-}m'q')\cdot\langle I||M_k||I\rangle\langle I||M_{k'}||I\rangle \qquad (5)$$

where the $J_{kk'}(\omega_{mm'})$ are the spectral density functions specifying the strength of the depolarizing interaction(s) at the transition frequency $\omega_{mm'}$ between the nuclear magnetic substates m and m'; the U_{kq} are the fluctuating components of the multipole potentials. The spectral density function is related to and derivable from the correlation function for the interaction, which must be developed based on the physical assumptions about the spin relaxation mechanism.

In making the tie to conventional nuclear magnetic resonance theory, it is important to remark that the experiments described here are all at low coverages, and we assume (more or less without proof) that the depolarization under discussion is the *spin–lattice* relaxation; spin–spin interactions are ignored for the present under the assumption that the mean residence time of the polarized adsorbate is less than the typical time between adsorbate collisions. (This last, incidentally, is one of the assumptions of the current model for spin relaxation that needs to be examined in the context of gas–surface collision theory. Even at low *average* coverages, this assumption may not hold true in the presence of steps, terraces, or other surface defects at which adsorbed impurities tend to accumulate.) It is also presumed in all of these discussions that the events of adsorption and desorption do not produce any alterations in the *nuclear* spin state of the probe atom. The main justification for this point of view is that the characteristic time scale for the nuclear polarization, measured in terms of the inverse of the Larmor precession frequency (10^{-6}–10^{-7} s), is 5 or 6 orders of magnitude slower than a vibrational period (10^{-12}–10^{-13} s), the characteristic time scale for electronic bonding or antibonding processes. However, recent calculations of gas–surface collisions suggest that charge transfer at

TABLE I. Representative Nuclear Polarization in an Alkali Atomic Beam Source[a]

spin 1 (^{6}Li)	N_1	N_0	N_{-1}	t_{10}	t_{20}	
WFT	0	$^1/_3$	$^2/_3$	−0.817	0.000	
SFT (3–5)	$^1/_3$	$^2/_3$	0	0.408	−1.225	
SFT (2–6)	$^2/_3$	0	$^1/_3$	0.408	1.225	
spin $^3/_2$ (^{7}Li, ^{23}Na)	$N_{3/2}$	$N_{1/2}$	$N_{-1/2}$	$N_{-3/2}$	t_{10}	t_{20}	t_{30}
WFT	0	$^1/_4$	$^1/_4$	$^1/_2$	−0.671	0.000	−0.224
SFT (2–8)	$^1/_2$	0	$^1/_4$	$^1/_4$	0.224	0.500	0.447
SFT (3–7)	$^1/_4$	$^1/_2$	0	$^1/_4$	0.224	0.000	−0.671
SFT (4–6)	$^1/_4$	$^1/_4$	$^1/_2$	0	0.224	−0.500	0.447

[a] The quantities N_i are the relative nuclear magnetic substate populations in the polarized beam. The various beam preparations are designated by the strength of the magnetic field (e.g., WFT for weak-field transition, SFT for strong-field transition) and the numbers in parentheses refer to the states whose populations are equilibrated by the transition, following the conventional labeling of the spin-1 or spin-$^3/_2$ Breit–Rabi diagram. (See Figure 4.)

metal surfaces may selectively populate certain electronic states, leading to interesting polarization effects caused solely by the desorption event—a prospect discussed in the last section of the paper.

IV. Experimental Concept and Apparatus

The use of spin-polarized nuclei in surface spectroscopy involves an interesting marriage of techniques from both nuclear and atomic physics. The essential elements of a nuclear surface physics experiment are the polarized atomic beam source, in which the atoms are prepared in a well-defined polarization state; the surface interaction region, where the polarized nuclei are perturbed by the surface itself and (sometimes) by external fields; and the detection apparatus that measures the polarization of the probe atoms after they are desorbed from the surface. We now consider each of these major elements of the experiment separately.

A. Rf Atomic Beam Source

In all the experiments described here, the source of nuclear-spin-polarized atoms is an atomic beam source of classical design, using a combination of multipole magnets and adiabatic rf transitions in a magnetic field to produce the polarization. Atomic beam sources of this type can be used to produce beams of alkali metals ^{6}Li, ^{7}Li, and ^{23}Na with particle currents ranging up to 10^{11} s^{-1}. A line drawing of such a source is shown in Figure 3. The atomic alkali vapor is produced by evaporating lithium or sodium metal in a small stainless steel oven. The thermal beam effuses through a nozzle and skimmer combination into a six-pole separation magnet, which radially focuses atoms with one electron spin while radially defocusing atoms with the opposite spin. Polarization of the atomic *nuclei* is achieved by one or more adiabatic radio-frequency transitions in a magnetic field following the sextupole magnet. In a more recent version of the atomic beam source designed specifically for surface physics experiments, the use of permanent magnets and other refinements has permitted drastic reductions in size and complexity.[13]

As an example of the way the source operates to polarize a beam of alkali atoms, we consider a spin-$^3/_2$ nucleus (e.g., ^{7}Li or ^{23}Na). The splitting of the levels in the static magnetic field of the transition section is shown in Figure 4. Since the states with $m_J = -^1/_2$ are defocused by the sextupole magnet, the atomic states labeled 1–4 in Figure 4 are the only ones populated at the entrance to the transition section. Rf transitions induced at magnetic fields much smaller than the

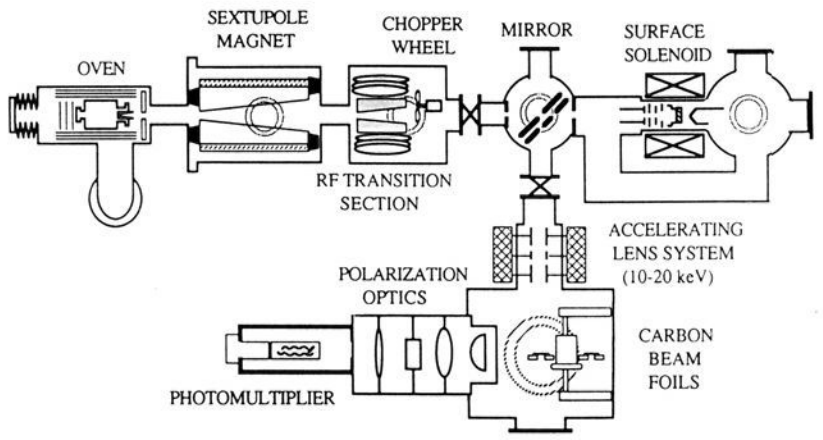

Figure 3. Plan view of a polarized alkali atomic beam source.

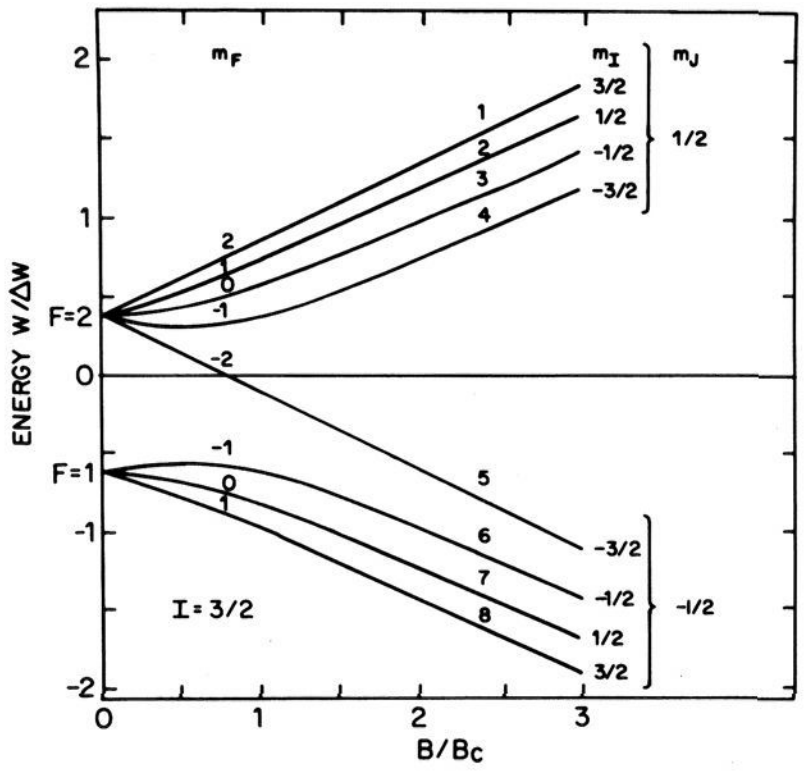

Figure 4. Energy-level diagram for an atom with nuclear spin $^3/_2$ and electron spin $^1/_2$ in a magnetic field. The magnetic field is given in units of the *critical field*, which is the value of the field at which the hyperfine interaction energy equals the dipole energy of the nucleus.

critical field B_c—the so-called "weak-field" transitions—interchange populations of states with magnetic quantum numbers m_F and $-m_F$. In stronger magnetic fields, on the other hand, one can introduce transitions between particular states (at the cost, of course, of higher radio frequencies), and one speaks of "X–Y strong-field transitions" that equalize the populations of states X and Y. The polarizations achievable for some representative rf transitions are shown in Table I; compared to typical polarizations of a few parts in 10^7 achieved with high magnetic fields in bulk samples, these polarizations are essentially unity. It should also be noted that by adding a second transition section,

it is possible to combine transitions, such as a weak-field and a particular strong-field transition, to achieve higher polarizations.

B. Surface Interaction Region

In the experiments carried out to date, the surface to be probed has been a polycrystalline or single-crystal transition metal. The surface sample, typically about 1 cm in diameter, is suspended by wires from tantalum supports and heated by the feedback-controlled current of a small electron gun located behind the surface. The surface temperature is measured by a pair of thermocouple wires passed against the surface; the thermocouple current can be used to control the filament current in the electron gun and thus provide a feedback-stabilized electron current to the sample. The surface temperature can be cross calibrated by an optical pyrometer, and the feedback circuit for the gun current maintains the temperature to within ±2 K of the desired set point. The surface sample also sits between wire loops that provide the alternating B field for NMR experiments. The entire assembly is mounted inside the bore of a large solenoid magnet that provides the guide magnetic fields (up to 300 mT) required to define the quantization axis for the beam polarization. The guide field B_0 preserves the nuclear spin during its flight to the surface by decoupling the nuclear and valence electron spins.

At the sample—generally a transition metal in the experiments described here—the spin-polarized adatom sticks at a distance from the surface that is characteristic both of the surface and of the probing atomic species. Since the technique used for removing the polarized probe atoms or ions from the surface is simple thermal desorption, the interaction time in these experiments is determined by the surface temperature and is given by an Arrhenius relation of the form

$$\tau = \tau_0 \exp[Q_d/k_B T] \tag{6}$$

where τ_0 is a characteristic time (of order 10^{-13} s) and Q_d is the activation energy for desorption (of order 3–4 eV for transition metals and alkali adatoms). The interesting range of interaction times—the range over which the polarization changes from fully preserved to fully destroyed—varies from fractions of milliseconds to as long as many seconds (in the case of ^{6}Li). This corresponds to temperatures on tungsten, for example, between about 1000 and 1800 K.

At any given surface temperature, a fraction of the adsorbed probe atoms N_+/N_0 given by

$$\frac{N_+}{N_0} = \frac{1}{2} \exp\left[-\frac{I-\phi}{k_B T}\right] \tag{7}$$

will desorb as ions, where ϕ is the work function of the surface and I is the ionization energy for the probe atom. Thus nuclear surface physics based on ion detection (via beam-foil spectroscopy) is limited by count-rate considerations to surfaces with high work functions; indeed, the necessity for measuring on oxygen-dosed surfaces in many of the early experiments arose directly from count-rate considerations. However, no such limitation applies to the desorbing *neutral* species—one more reason, of course, for the measuring their surface-induced depolarization instead.

C. Polarization Detection for Desorbed Ions and Atoms

The detection of the nuclear polarization for ions occurs via beam-foil spectroscopy.[14] The ions are accelerated away from the surface by means of an electrostatic lens system at a potential of a few kilovolts; they are then deflected into a beam-foil chamber by an electrostatic mirror. In the beam-foil chamber, the ions are accelerated to 10–20-keV energy and pass through a thin carbon foil, in which a large fraction capture an electron in an excited state. Downstream from the foil, the electron interacts with the nucleus via the hyperfine interaction and acquires a polarization proportional to the nuclear polarization. The polarization of the radiation emitted by the electron when it decays to the ground state is a measure of the nuclear polarization at the time of the electron capture. Because the time of flight between the surface and the beam foil is short compared to the nuclear depolarization time for the ion, this optical polarization is also diagnostic for the nuclear polarization at the time of desorption. While the beam-foil process is relatively inefficient, the measured photomultiplier count rates are still on the order of 5×10^4 counts/nA of ion current, so that measurement times remain reasonable even for surface ionization efficiencies near 0.1%. Moreover, since the measured effect is a ratio of counting rates, certain systematic errors cancel, allowing measurements with high precision.

The polarization of desorbed neutral atoms is determined by passing them through a region of space containing a uniform magnetic field that effects a Zeeman splitting into the different magnetic sublevels of the nuclei. The polarization is measured by using laser-induced fluorescence to monitor the relative populations of atoms in different magnetic substates, using standard optical detection techniques.[15,16] This detection scheme, of course, is just the inverse of optical pumping schemes for preparing polarized beams in a single magnetic substate, as discussed in section VI. A comparison of the diagnostic signals from an unpolarized beam, a partially polarized beam, a beam prepared in a single magnetic sublevel, and a sample of nuclei desorbed from a surface is shown in Figure 5.

D. Interpretation of the Experimental Data

In the experiments done to date, a continuous beam of polarized atoms is produced in the source and impinges on the surface, so that the observed depolarization is an average over the residence (interaction) time of the polarized probe on the surface. It can be shown[4] that for a given residence time τ and constant atomic beam intensity, the ith component of the polarization of the desorbing nuclei can be expressed as

$$P^i(\tau) = \frac{1}{\tau}\int_0^\infty P^i(t) \exp(-t/\tau)\, dt = \frac{P_0^i}{\alpha^i \tau + 1} \tag{8}$$

where α^i is a relaxation rate (analogous to the spin–lattice relaxation rate $1/T_1$ in conventional NMR). Thus a simultaneous determination of the mean residence time through a measurement with an unpolarized beam and of the polarization of the beam-foil radiation using a polarized beam can yield the relaxation rates $\alpha^i(T)$. In general, of course, all the ranks of polarization

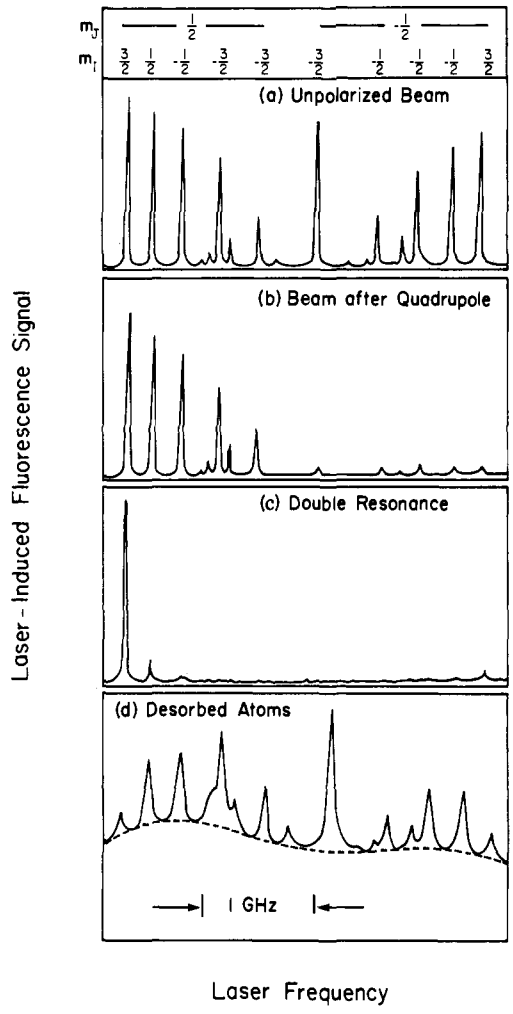

Figure 5. Nuclear spin measurements using laser-induced fluorescence in a magnetic field. The spectra in (a), (b), and (c) are for measurements on an atomic beam prepared in various ways: (a) unpolarized; (b) electron-spin polarized by a quadrupole magnet; and (c) fully polarized (single magnetic substate) by applying an rf field while pumping with circularly polarized laser light. The bottom spectrum (d) comes from a laser-induced fluorescence measurement on a partially polarized ensemble of atoms desorbed from a tungsten surface. Adapted from ref 13, 16, and 40.

are coupled; however, because of the flexibility in choosing the polarization state of the incident beam, it is generally possible to make all but one of the α^i negligibly small. For nuclear level mixing and nuclear magnetic resonance experiments where one wishes to minimize the effects of the spin relaxation, one can generally choose T sufficiently large that $\alpha^i(T)$ is negligible on the time scale of interest. It is to be emphasized that the measured depolarization rates α^i are characteristic of a coupled adsorbate–surface system, and not of the surface in isolation, since both the residence time and the average bond length at the surface vary with adsorbate and surface characteristics.

V. Surface Analysis Experiments

Three generic nuclear surface physics experiments have been carried out thus far using the polarized-beam techniques described above: nuclear spin relaxation (NSR) measurements, in which the spin relaxation process is dominated by the randomly fluctuating fields encountered by the nucleus as it hops about on the hot

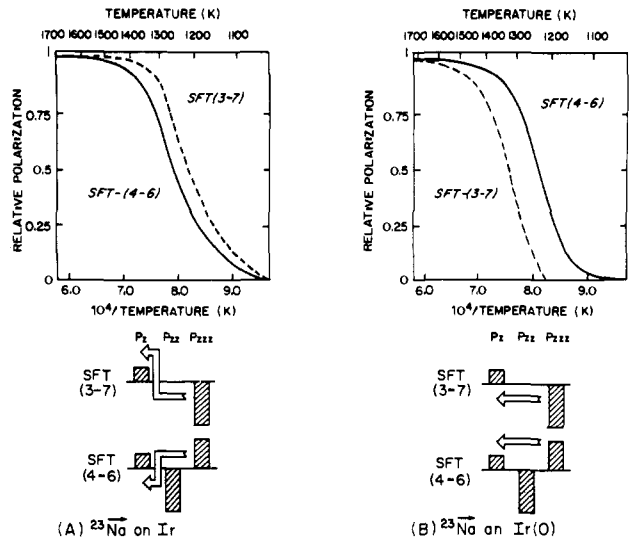

Figure 6. (A) Vector polarization as a function of temperature for a polarized ^{23}Na nucleus on an Ir surface. The two curves are for two different preparations of the atomic beam (see Table I). (B) Vector polarization as a function of temperature for a polarized ^{23}Na nucleus on an Ir/O surface (approximately monolayer coverage) for the same two preparations of the incident atomic beam. In both spectra, the relative incident beam polarizations (in the Cartesian representation) are indicated below the polarization vs temperature curve.

surface, and nuclear magnetic resonance (NMR) and nuclear level mixing (NLM) experiments, in which the time variation of the perturbing potential is essentially static on the scale of the nuclear hyperfine frequency. Here we are concerned simply with presenting the general features of recent significant experiments and discuss their implications for the future development of a generalized surface analytical capability based on nuclear-spin-polarized atomic beams.

A. Spin Relaxation Experiments: Adsorbate Effects

The earliest NSR experiments showed that the dominant process involved some sort of thermally activated depolarization mechanism.[4] Figure 6, for example, shows the temperature dependence of the vector polarization of ^{23}Na on a polycrystalline Ir surface ionizer for different beam and surface preparations. The characteristic features of these curves are easily explained in a qualitative way: At low temperatures (long mean residence times), the nucleus is completely depolarized prior to desorption because of the large number of interactions with the fluctuating field gradients in the surface. At higher temperatures (shorter mean residence times), on the other hand, ionization takes place before complete depolarization, and hence the nuclear polarization of the desorbing ion increases; at sufficiently high temperatures, in fact, the polarization of the incident nuclei is completely preserved in the desorbing ions. In between these two extremes of residence (or interaction) times with the surface, the polarization changes as a function of temperature in accordance with eq 8.

The temperature dependence of the mean residence time can be evaluated by using a mechanically chopped unpolarized beam and the beam-foil detector to measure the exponential drop in desorption yield as a function of time after the beam is turned off. *If* the

relaxation is due to a single interaction, so that the relaxation is characterized by a single rate constant α, then a simultaneous measurement of mean residence time and time-averaged polarization at the same temperature gives this relaxation rate unambiguously. Even if more complex mechanisms are at work, it is often possible to calculate the different α^i by simultaneously measuring and fitting both the first- and second-rank polarizations under identical surface conditions.[17]

In NSR experiments the only external field is that which defines the quantization axis and it is held constant during the experiments. Hence, changes in the density matrix arise from the relaxation terms that contain the fluctuating component of the time-dependent surface fields $V_{kq}(t)$. There are several obvious candidates for the source of the fluctuating field gradients that lead to the observed spin relaxation, including electronic fluctuations, lattice vibrations, adsorbate oscillations, and surface diffusion. Of these, the only one that has a time constant close to the characteristic nuclear time constants is surface diffusion. Since the rate equation for the relaxation component of the density matrix contains a spectral density function that measures the strength of the interaction between the reservoir and spin system atoms *at the transition frequency* between the various spin states, we conclude that surface diffusion is the most likely depolarization mechanism. This choice has to some extent been confirmed in the measurements described in section V.D.

The time dependence of the depolarization can be computed from the density matrix by using eq 1–5, yielding a set of coupled differential equations relating the time history of a given polarization t_{k0} (which is proportional to the asymmetry effects measured with the beam-foil apparatus) to the values of the other polarizations and to the surface fields. These latter are of course contained in the transition probabilities $W_{mm'}$.

Repeated measurements with different combinations of polarized probes and surfaces have shown that the relaxation rate depends exponentially on $1/T$, where T is the absolute temperature. From this fact, we infer that the dynamical mechanism causing the spin relaxation must (1) have an inverse correlation time $1/\tau_c$, which is closer than other competing mechanisms to the transition frequencies between spin states, and (2) have an exponential dependence on $1/T$. Surface diffusion is a likely mechanism because the hopping frequencies for alkali diffusion on metal surfaces at 1300 K are of order 10^{10} Hz, much smaller than the frequencies of lattice vibrations (10^{12} Hz) or electronic fluctuations (10^{16} Hz). Moreover, the jumping rate is known to obey an Arrhenius relation of the form

$$\Gamma = \Gamma_0 \exp[-E_{\text{diff}}/k_B T] \tag{9}$$

Hence, a fit of the depolarization curves yields not only a relaxation rate but also a value for the activation energy of the diffusion process. The diffusion energy E_{diff} extracted from experiments with polarized Na on Rh is, for example, a few tenths of an electronvolt. It should be noted, however, that these values for the diffusion energy are derived by estimating the jumping rate. Values for the prefactor Γ_0 have to be derived from measurements of absolute diffusion rates—which is, in general, a much more difficult experiment now done usually by techniques of field ion microscopy,[18] but which also may be possible by carrying out these experiments in a variable guide magnetic field, as discussed in section V.F.

Nuclear spin relaxation studies can yield information on the relative sizes of differing components of the fluctuating surface fields if one makes use of the variety of polarization states available from the atomic beam source. (See Table I for some examples.) For a spin-$^3/_2$ particle, for instance, the rate equation for the vector polarization t_{10} can be derived from eq 9 and turns out to be

$$\left(\frac{h^2 J(\omega)}{4\pi^2}\right)\dot{t}_{10} = -t_{10}\left\{\frac{4}{9}\mu^2|V_{11}{}^2|^2 + \frac{1}{5}(eQ)^2[|V_{21}|^2 + 4|V_{22}|^2]\right\} + t_{20}\left(\frac{4}{15^{1/2}}\mu(eQ)V_{21}V^*{}_{11}\right) - t_{30}\left(\frac{2}{5}(eQ)^2[|V_{21}|^2 - |V_{22}|^2]\right) \tag{10}$$

For a nuclear probe with a large quadrupole moment, e.g., ^{23}Na, the term containing μ^2 is negligible compared to those terms containing the quadrupole moment. Moreover, by choosing a beam preparation with a small second-rank polarization t_{20}, one can effectively get rid of the second term in eq 10 as well. Hence, it is possible to measure the relative strengths of V_{21} and V_{22}—which are respectively the in-plane and out-of-plane components of the fluctuating electric field gradient—by measuring the changes in the depolarization rate for differing beam polarizations.

Parts A and B of Figure 6 illustrate the results of such an experiment, in which a beam of ^{23}Na atoms prepared in two different ways (SFT 3–7 and SFT 4–6 transitions, respectively) was incident first on a polycrystalline Ir surface and then on an Ir/O surface. In Figure 6A, the surface is clean and the vector polarization of atoms with the SFT 3–7 beam preparation relaxes faster than the atoms prepared in the SFT 4–6 state. Examination of rate equation (10) shows that this can only occur if $|V_{21}|^2 > |V_{22}|^2$. On the other hand, in Figure 6B, where the Ir crystal has oxygen coverage at about the monolayer level, the situation is just the reverse: $|V_{21}|^2 < |V_{22}|^2$. Indeed, the ratio of these two components of the fluctuating field gradient can be taken as an accurate quantitative measure of changing surface conditions.[19] Since the *absolute* value for the field gradients experienced by the coupled adsorbate–surface system depends only on the square root of the correlation time τ_c, it is also possible to extract reasonably accurate absolute magnitudes for both in-plane and out-of-plane components using estimates of the jumping rate.[20]

Attempts to fit these data into a model of interactions with magnetic vs electric field gradients were inconclusive. Comparisons of the relaxation rates of ^{6}Li and ^{7}Li showed that they scaled approximately with the square of the magnetic moment ratio; however, the estimated quadrupolar relaxation rate for ^{7}Li was of roughly similar magnitude as the measured dipolar relaxation rate. Hence it appears premature to try to connect these results with models based on the differences between the Knight shift and the quadrupole interaction. Since these measurements were made un-

der less than ideal vacuum conditions, it will probably be necessary to repeat them to verify that spin relaxation data can be related in a reproducible way to surface composition and electronic structure.

B. Nuclear Level Mixing Experiments

The NSR measurements yield values for the mean-square values of the fluctuating field gradients arising from the fast diffusive motion of the polarized nucleus over the heated surface. With level mixing (NLM) and magnetic resonance (NMR) experiments, we move into a regime where the depolarizing fields have time scales long compared to $1/\omega_L$ and where one tries in general to choose a surface temperature sufficiently high that relaxation phenomena are no longer dominant. In both NLM and NMR measurements, the measured quantities are not the *fluctuating* field gradients but rather the *average* field gradients experienced by the nucleus, so both measurements yield similar information. However, because of the characteristic differences in the spectral line shapes arising from NMR and NLM measurements, the choice of a suitable operating temperature to minimize relaxation effects may favor one or the other technique in a given circumstance.[21]

As an example of the information obtainable through an NLM experiment, we discuss the results obtained with nuclear-spin-polarized ^{23}Na chemisorbed on a clean and on an oxygen-covered W(110) surface. The Hamiltonian for a nucleus with both a dipole and a quadrupole moment in a magnetic field B_z is[10]

$$\mathcal{H} = \mathcal{H}_D + \mathcal{H}_Q = -\gamma B_z \mu I_z + eQV_{zz}\left[3I_z^2 - I(I+1) + \frac{\eta}{2}(I_+^2 + I_-^2)\right] \quad (11)$$

where γ is the gyromagnetic ratio, μ is the dipole moment, (eQ) is the quadrupole moment, and I, I_z, and $I_\pm$ are the usual angular momentum operators. The quantity η is the asymmetry parameter

$$\eta = (V_{xx} - V_w)/V_{zz} \quad (12)$$

and represents the strength of the non-axially-symmetric component of the quadrupole interaction. The vector polarization of the spin-$^3/_2$ ^{23}Na nucleus is

$$t_{10} = \left(\frac{9}{5}\right)^{1/2}\left[(N_{+3/2} - N_{-3/2}) + \frac{1}{3}(N_{+1/2} - N_{-1/2})\right] \quad (13)$$

where the N_i are the relative populations of the four magnetic substates of this nucleus. The level scheme for a spin-$^3/_2$ nucleus interacting with a static magnetic field is shown in the upper portion of Figure 7. For $B_z = 0$ the energy levels are split by the quadrupole interaction; at higher values of the field the degeneracy of the $|m| = {}^3/_2$ and $|m| = {}^1/_2$ levels is removed by the magnetic dipole interaction (ordinary Zeeman splitting). These Zeeman levels cross at two values of the magnetic field: first at $B_z = 3\omega_Q I/\mu$ (for $\Delta m = \pm 2$, where the $m = {}^3/_2$ and $m = -{}^1/_2$ levels intersect), and then again at $B_z = 6\omega_Q I/\mu$ (where the $m = {}^1/_2$ and $m = {}^3/_2$ levels cross and $\Delta m = \pm 1$). If η were vanishingly small, the energy levels of the polarized nucleus in a magnetic field would appear as the solid lines in Figure 7. Although the levels cross at the indicated values of the magnetic field, if

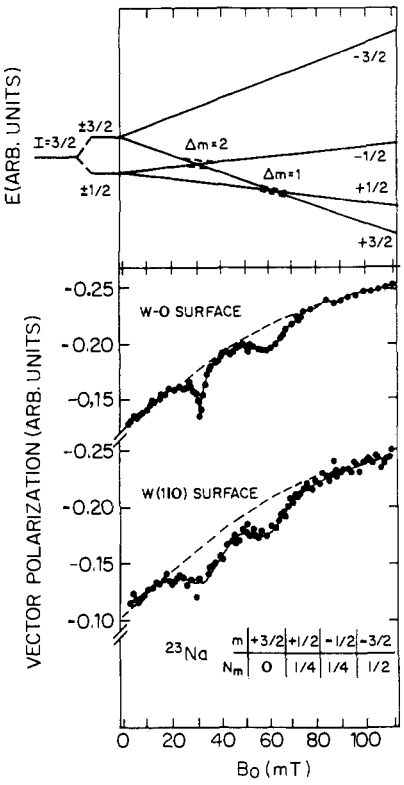

Figure 7. Upper diagram: Zeeman effect for a spin-$^3/_2$ nucleus in the presence of an electric field gradient. At the level crossings, mixing of different initial polarization states can occur. Lower diagram: Vector polarization of ^{23}Na ions desorbing from a clean and from an oxygen-covered W(110) surface as a function of external magnetic field strength. The inset shows the relative occupation numbers of the nuclear magnetic substates in the incident beam.

only the $q = 0$ terms contribute to the Hamiltonian, the original eigenstates of the system will be preserved. However, for finite values of η, the Hamiltonian will contain terms with $q \neq 0$ and the degeneracy of the levels at the crossing points will be removed.

Thus, for example, in this experiment on the W(110) surface (which has only twofold rather than complete axial symmetry), there will be contributions to the polarization from terms with $q = \pm 2$; namely

$$V_{2\pm 2} = \frac{1}{2(6^{1/2})}(V_{xx} - V_{yy}) = \frac{1}{2(6^{1/2})}\eta V_{zz}$$

$$M_{2\pm 2} = (eQ)I_\pm^2\left[\frac{6^{1/2}}{4I(2I-1)}\right] \quad (14)$$

Due to the conservation of angular momentum, this interaction can only influence the first-level crossing, where $B_z = 3\omega_Q I/\mu$ and $\Delta m = \pm 2$. If the surface normal is tilted with respect to the external field defining the quantization axis of the system, on the other hand, the Hamiltonian will contain terms involving $V_{1\pm 1}$; in that case, there will be a change in the polarization at the second-level crossing, where $B_z = 3\omega_Q I/\mu$ and $\Delta m = \pm 2$. In this experiment, the tilt angle of the surface was 5.2°. The dashed lines in the upper portion of Figure 7 represent qualitatively the removal of the level degeneracy at the two crossing points.

The changes in polarization at the crossing points are proportional to the non-axially-symmetric part of the Hamiltonian **H**—i.e., the terms containing the asymmetry parameter and the tilt angle. The magnetic field

at which the crossings occur determines the axially-symmetric part of the EFG tensor, V_{zz}.

The lower part of Figure 7 shows the vector polarization of ^{23}Na ions desorbing from a clean and from an oxygen-covered W(110) surface as a function of the external magnetic field. In addition to the two pronounced "resonances" at B = 30 mT and at B = 60 mT, one also observes a smooth increase of the polarization as a function of the external magnetic field. This effect arises from the mixing of atomic levels by the hyperfine interaction and the consequent changes in nuclear polarization as the beam approaches the surface region and the external magnetic field.

It will be noted that for both clean and oxygen-covered surfaces, the "resonances" occur at the same magnetic field strength, indicating that V_{zz} is the same for both surfaces; the extracted value is approximately -5×10^{16} V/cm^2. Since the tilt angle was the same for both measurements, the two "resonances" at the upper level crossing should appear identical, as in fact they do. However, the pronounced differences between the shapes of the two lower field resonances indicate that the asymmetry parameter for the EFG tensor must change significantly with the addition of oxygen. A fit to the data yields η = 0.08 and 0.02 for clean and oxygen-covered W(110), respectively. By comparing the NLM data with NMR results for ^6Li, ^7Li, and ^{23}Na for these two surfaces, it has been possible to measure both in sign and magnitude of the average EFG with changing distance from the sample surface.[15,16]

C. Nuclear Magnetic Resonance Experiments

Perhaps the most intuitively attractive of the surface physics experiments made possible by polarized-beam techniques are nuclear magnetic resonance studies on single-crystal surfaces.[22,23] Two examples from recent experiments will illustrate the application of this variation of NMR methods, both dealing with polarized lithium nuclei on tungsten surfaces.

At the temperatures characteristic of present nuclear surface physics experiments (1000–1800 K), the mean residence time of the lithium atoms on the surface ranges from 1 to 10^{-3} s. During this time, the nuclear moments of these atoms interact with the EFG generated by the electronic charge distribution in their immediate environment, with the external static field, and with the applied rf fields. There is also a fluctuating component of the EFG generated by the surface diffusion of the adsorbed atoms, for which the correlation time is of order $\tau_c = 10^{-10}$ s (the inverse of the hopping rate at 1300 K). However, this is significantly shorter than the inverse of the Larmor frequency in these experiments, for which B ranges between 0.01 and 0.1 T and $\omega \sim 0.1$ MHz. Thus the fluctuations of the EFG are rapid compared to the characteristic depolarization times for the adsorbed nuclei and we are always in the regime of extreme motional narrowing[9] where one measures an *average* EFG. Nevertheless, the fluctuations in the EFG do relax the polarization, and the surface temperature is thus constrained to relatively high values (i.e., short mean residence times) in order to minimize this depolarization. The precise choice of temperature is a judicious compromise between the desirable spectral line shape produced by motional narrowing and the saturation of the NMR transition

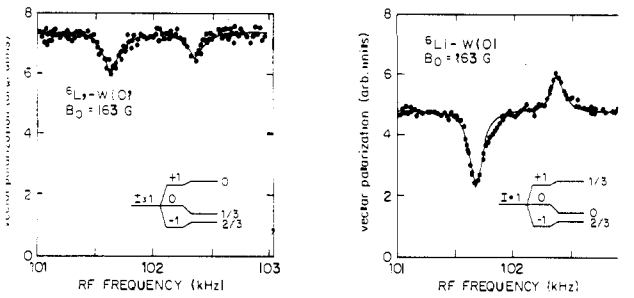

Figure 8. NMR spectra of ^6Li on an oxygen-covered W(110) surface for two different preparations of the incdient atomic beam. The Larmor frequency is 102.1 kHz. The insets refer to the relative magnetic substate populations of the nuclei in the incident beam.

caused by a sufficiently long residence time on the surface.

For a spin-1 nucleus—e.g., ^6Li—the vector polarization is related to the relative magnetic substate populations by

$$t_{10} = (3/2)^{1/2}(N_{+1} - N_{-1}) \tag{15}$$

The Hamiltonian $\mathcal{H}$ for the "static" interaction of the adsorbed lithium in the surface is the same as that displayed earlier in eq 12. However, the oxygen-covered tungsten surface has axial symmetry, so that only terms with q = 0 contribute to the Hamiltonian:

$$M_{10} = (\mu \cdot I_z)/I \qquad V_{10} = B_z \tag{16a}$$

$$M_{20} = (e \cdot Q)\left[\frac{3I_z^2 - I(I+1)}{2I(2I-1)}\right] \qquad V_{20} = V_{zz}/2 \tag{16b}$$

The normal Zeeman effect on a spin-1 system subjected to an rf field would produce a single resonance line at the Larmor frequency ω_L. However, the quadrupolar interaction with the EFG splits this resonance line into a doublet at the frequencies $\omega_+ = \omega_L + 3\omega_Q$ and $\omega_- = \omega_L - 3\omega_Q$, where the quadrupole frequency ω_Q is the same as that defined earlier.

Figure 8 shows NMR spectra of ^6Li adsorbed on W–O, with each spectrum showing the expected doublet of resonance lines for a nucleus interacting with both the static field B_0 and an average EFG. (As remarked before, the use of oxygen in this case is a device for increasing the ion yield for the beam-foil measurement of the nuclear polarization following the surface interaction.) The measured splitting in the upper curve of about 720 Hz corresponds to an EFG component V_{zz} = 3.08 (8) $\times 10^{15}$ V/cm^2 (given the ^6Li quadrupole moment of Q = 0.8 e mb). The differences between the upper and lower spectra arise from the differing preparations of the m-substate population of the incident atomic beam. In the lower spectrum, rf transitions between the m = 1 and m = 0 substates causes an increase of the polarization, while the transition from m = 0 to m = 1 causes a decrease. The ordering of these transitions as a function of frequency determines the sign of V_{zz}; in this case, if one examines the symmetric part of the Hamiltonian, it becomes evident that this ordering of the doublet implies that V_{zz} must be negative. Similar experiments carried out with ^{23}Na indicate that the field gradient actually changes sign at greater distances from the surface. NMR experiments on clean

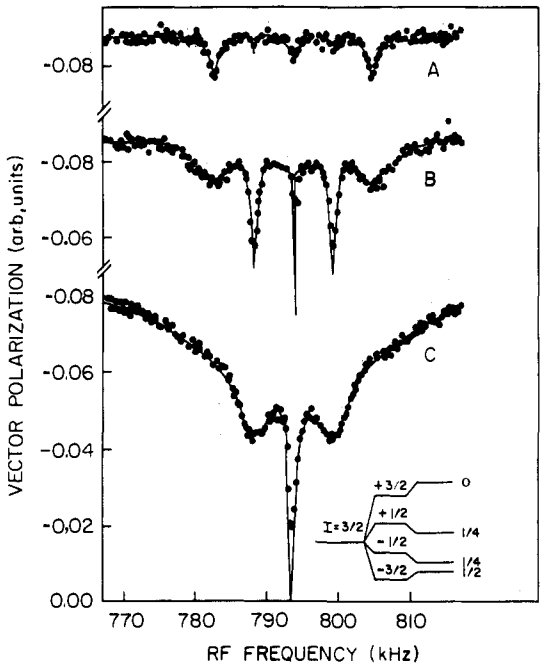

Figure 9. NMR spectra for ^{7}Li on an oxygen-covered W(110) surface, demonstrating the occurrence of multiple-quantum or multiphoton transitions as the rf power level at the surface is increased. The rf power increases from the top to the bottom curves.

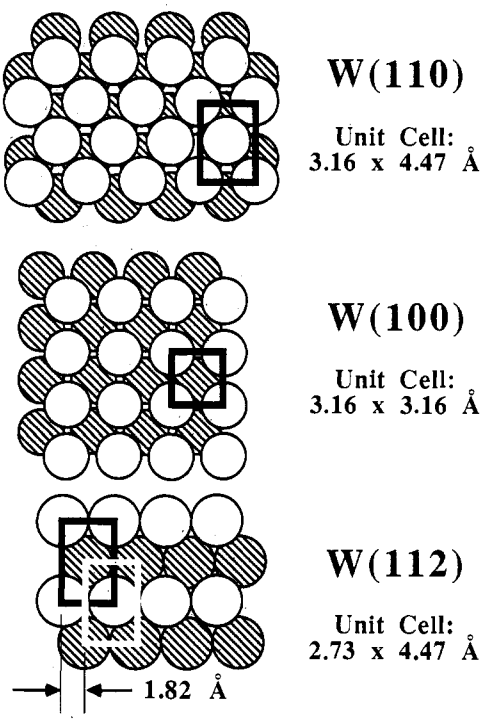

Figure 10. Hard-sphere model of various tungsten single-crystal surfaces: W(100), the most symmetrical of the surfaces; W(110), the most closely packed; and W(112), a highly asymmetric surface.

W(110) surfaces also confirm the asymmetry parameters measured in the level-mixing experiments cited above.[23]

Another striking result of the early NMR experiments is a demonstration of multiple-quantum transitions for polarized ^{7}Li nuclei (spin-$^3/_2$) on the same W(O) surface. The vector polarization of the beam t_{10} can be computed from the initial magnetic substate population indicated in the inset of Figure 9 by using eq 15. In the uppermost spectrum, taken at low rf power levels, one sees two $\Delta m = 1$ resonances at the extremes flanking the Larmor line in the center and the barely discernible $\Delta m = 2$ transitions. In the middle spectrum, taken at an intermediate rf power level, the one-quantum transitions have broadened considerably, while the two- and three-quantum transitions are now the dominant feature. The lowermost spectrum was obtained with the highest rf power level. In this spectrum, the broad shallow structure running almost completely across the spectrum is actually a superposition of the three $\Delta m = 1$ transitions, which are run together because of power broadening from the rf source. The two sharper resonances flanking the central downward spike are the $\Delta m = 2$ transitions; this identification is confirmed by a calculation of the level splittings indicated in the figure. The sharp spike is indeed the $\Delta m = 3$ transition, identifiable as such because the polarization can only vanish if the populations of the $m = {}^3/_2$ and the $m = -{}^3/_2$ levels are equilibrated by the induced rf transitions.[24] Here again one sees the inherent power of using a probe whose polarization can be both specified in and varied by a source of nuclear-spin-polarized atoms.

D. Effects of Varying Crystal Surfaces in NMR and NLM Studies

Because of the variety of possible effects on the spin-polarized nucleus, including the effects of diffusion over a relatively broad region of the surface during the long residence times, it is important to be able to compare magnetic resonance and level-mixing data on a variety of different surfaces of the same metal. It is difficult to do this, however, as long as ion detection is used, since variations in work function strongly effect the ion yield (see eq 7). This difficulty has been overcome in some recently published experiments by Memmert and Fick[25] using laser-induced fluorescence polarization measurements on desorbing alkali *atoms* from several different tungsten single-crystal surfaces: W(110), the most closely packed surface; W(100), the most symmetric surface; and W(112), a low-index, highly asymmetric surface. The three geometries are shown in Figure 10.

Even more interesting is the fact that, with neutral-atom detection, it is possible to measure and compare the shifts in the positions of the NMR peaks as a function of adsorbate-induced changes in the surface electronic structure—analogous to the chemical shift that is the keystone of NMR measurements in solids and liquids. Figure 11 shows the shifts in peak positions for the three measurable $\Delta m = 1$ transitions for ^{23}Na nuclei on W(100) and W(112) surfaces as a function of time following flash heating of the tungsten crystal to approximately 2000 K. Because the vacuum in the sample chamber for these experiments was only of order 10^{-9} Torr, one can assume that immediately following the flash heating process, residual gases in the chamber begin to stick on the surface, changing the electromagnetic environment of the adsorbed polarized ^{23}Na nuclei. On the symmetrical W(100) surface—as, indeed, on the W(110) close-packed surface as well—the central Larmor peak is unshifted following the flash; however, the two outer peaks in the spectrum shift toward the Larmor peak and finally exchange positions on the W(100) surface, while on the W(112) surface the two outer peaks move asymmetrically toward each other

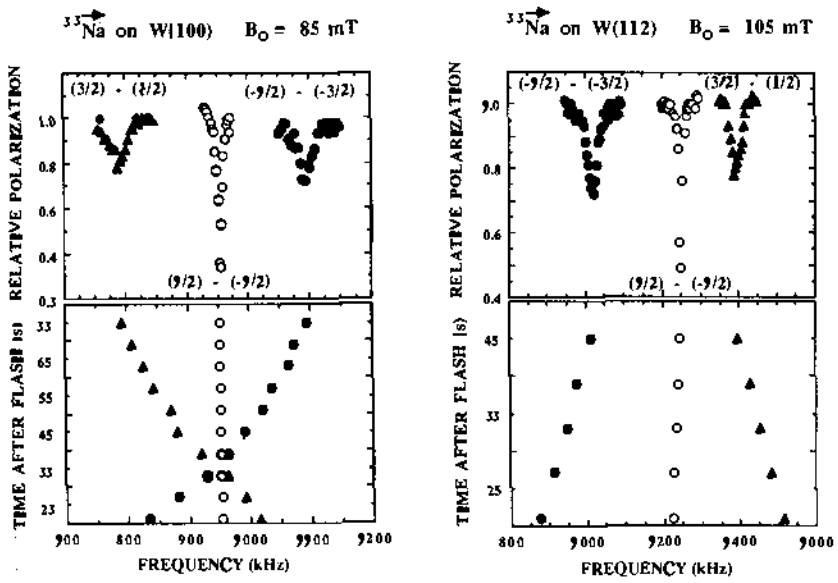

Figure 11. NMR spectra for polarized Na atoms W(100) and W(112) surfaces, respectively. The upper spectrum in each case is for the equilibrium condition of the surface. The lower spectrum shows how the position of the NMR peaks shifts after flash heating of the sample to 2000 K. Triangles refer to the $(^3/_2)$–$(^1/_2)$ transition; open circles to the $(^1/_2)$–$(^{-1}/_2)$ transition; and filled circles to the $(^{-1}/_2)$–$(^{-3}/_2)$ transition in each case. Adapted from ref 13 and 25.

and the central Larmor peak. The Larmor peak itself changes position slightly on the W(112) surface, in contrast to its behavior on the smoother (100) and (110) surfaces.

One significant question is: Do these shifts represent a chemical shift in the sense it is usually understood in the NMR community? Since the conventional chemical shift is a dipolar effect arising from spin–orbit coupling, the answer, in this case, is "no" in the narrowest sense, particularly in view of the fact that the ^{23}Na nucleus interacts with the surface primarily through its quadrupole moment. However, the shift in the positions of the quadrupole resonances does represent a measurable response to a change in the chemical environment of the adsorbate and, thus, with proper correlations to other surface measurements (LEED and Auger spectroscopy, for example) could be made to yield useful information on that "chemical shift".

E. Measurement of Local Density of States

One of the most recent successes of the polarized-beam spin resonance technique involves a measurement of the density of states at the Fermi surface of a metal from measurements of the spin–lattice relaxation as it varies with work function.[26] The problem of obtaining detailed measurements of the charge-transfer resonance between a chemisorbed alkali atom and a metal surface has been outstanding for many years, even though a qualitative understanding of the situation has existed since the first treatments by Langmuir[27] and by Gurney.[28] The general picture is shown schematically in Figure 12, where the shifting and broadening of the ionization level, I, of the adatom produce a resonance that extends below the Fermi surface of the metallic electron wave functions and allows charge transfer or hybridization by electron tunneling. The experimental method is essentially the same as that described earlier, except that to guarantee surface cleanliness, the temperature of the sample surfaces was raised between depolarization measurements by flash heating to approximately 2000 K, and the cleanliness of the surface was then checked by Auger electron spectroscopy. The

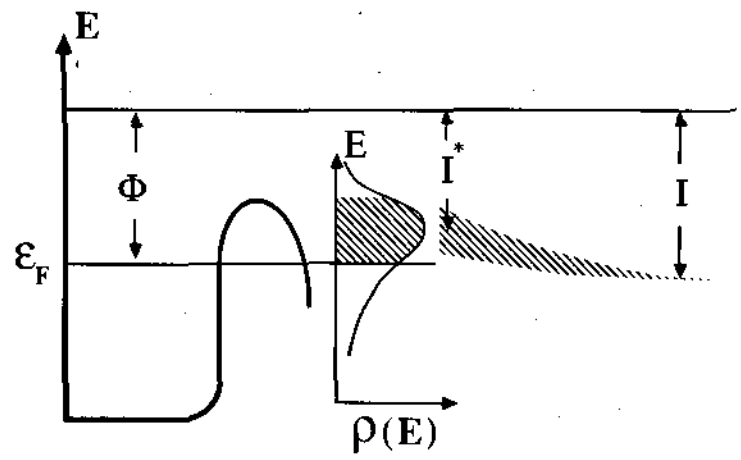

Figure 12. Level scheme for an adsorbed alkali atom on a metal surface, showing the changes in the first resonance level and the overlap with the Fermi surface.

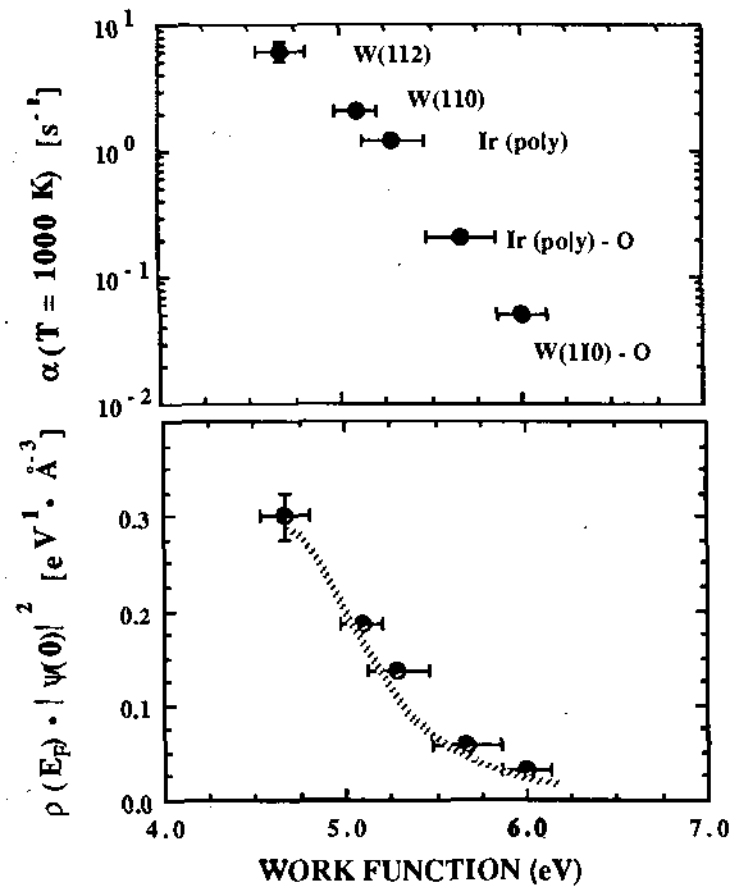

Figure 13. Experimental values for the density of states at the Fermi level for metals with different work functions (top); calculated values for the work function dependence of the density of states at the Fermi level, showing the effects of various values for the electron–gas parameters. The dashed curve is calculated assuming a Lorentzian form for the resonance. From ref 26.

relaxation rate was measured for several surfaces with differing work functions at a temperature of 1000 K, including W(112), W(110), Ir, Ir/O, and W(110)/O; in the case of measurements made with oxygen, the partial pressure of the O_2 in the ultrahigh-vacuum chamber was approximately 10^{-4} Pa. The relaxation rate, as computed from eq 8, varies linearly with temperature, hinting that the Fermi contact interaction between electron spins in the metal and the ^{6}Li nucleus is the depolarization mechanism, rather than the diffusion process observed for the other experiments described here. This mechanism allows electrons within $\approx kT$ of the Fermi level to interact with the hybridized 2s valence electron, leading to simultaneous spin flips of the nucleus and the 2s valence electron.

The experimental results are shown in the upper portion of Figure 13; note that while the range of variation of the work function is only about 1.5 eV for all the measurements, the measured relaxation rates range over some 2 orders of magnitude. The calculated relaxation rate for a Fermi contact interaction is

$$\alpha = \frac{512\pi^4}{9h}\mu_e^2\mu_N^2 kT\rho^2(E_F)\langle|\varphi(0)|^2\rangle^2 \quad (17)$$

where $\rho(E_F)$ is the density of s-state electrons at the Fermi energy, and the wave function $\varphi(0)$ represents the density of s electrons at the ^{6}Li nucleus. If one parametrizes the resonance $\rho[E_F(\Phi)]$ as a Lorentzian, it is possible to calculate ρ directly from the measured spin relaxation rate α at a given temperature. The smooth curve in the bottom of the figure is one such fit for a parameter set reasonably consistent with trends from Knight-shift experiments on Li in bulk solids.

F. Surface Diffusion Measurements

The measurement of surface diffusion of adatoms is one of the fundamental problems of surface science and a matter of enormous practical importance.[29,30] The role of surface diffusion as the major contributor to spin relaxation of adsorbed polarized nuclei was conjectured in the earliest papers on the subject,[4] but not verified until recently, when it became possible to consider measurements that might highlight spectral density functions of lower dimensionality than three.

That the spectral density function for a diffusive process should depend on the dimensionality of the surface can be seen from the following heuristic argument. The conditional probability $P_d(\mathbf{r}_0,\mathbf{r},t)$ that a spin be located at $\mathbf{r}$ at time t, provided it was at $\mathbf{r}_0$ for time $t = 0$, can be approximated by the well-known solution of the diffusion equation

$$P(\mathbf{r},\mathbf{r}_0,t) = \frac{1}{(8\pi Dt)^{d/2}}\exp\left[-\frac{|\mathbf{r}-\mathbf{r}_0|^2}{8Dt}\right] \quad (18)$$

where D is the diffusion constant and d the dimensionality of the system. Since the conditional probability for the diffusion process enters into the spectral density function for the depolarization through the Fourier transform of the correlation function (see Appendix, eq A.8 and A.9), the depolarization must depend on the dimensionality d of the diffusion process.

The low-frequency (that is, high-temperature) limits ($\omega \ll 1$) of the spectral density function have been calculated for the various dimensionalities to be[31-33]

$$d = 3 \qquad J(\omega) \rightarrow \tau_c \quad (19a)$$

$$d = 2 \qquad J(\omega) \rightarrow \tau_c \ln[1/\omega\tau_c] \quad (19b)$$

$$d = 1 \qquad J(\omega) \rightarrow \tau_c/(\omega\tau_c)^{1/2} \quad (19c)$$

where τ_c is the correlation time. Clearly, $J(\omega)$ diverges in the low-frequency limit for $d = 1$ and 2. The effective relaxation rate $\alpha(T)$ depends linearly on certain combinations of transition matrix elements $W_{mm'}$, which themselves depend on the spectral density function. Also, the frequency scale for the nuclear spin precession—namely, the size of the Larmor frequency for a given nucleus—is set in these experiments by the size of the guide magnetic field. Hence, even without specifying *explicitly* the dependence of the effective relaxation rate on the individual matrix elements, we know that α also has to follow the frequency (i.e., magnetic field) dependence appropriate to the d-dimensional diffusion. Thus we conclude that an increasing nuclear spin relaxation should be observed for a decreasing Larmor frequency or, equivalently, for a magnetic field approaching zero at the sample surface.

The basic features of the experiment were similar to others described here. A thermal velocity, nuclear-spin-polarized ^{7}Li atomic beam impinged on a hot oxygen-covered W(110) surface. The m-substate populations of the beam as prepared in the source were $N_{+1/2} = N_{-1/2} = +^1/_4$, $N_{-3/2} = {}^2/_4$, and $N_{3/2} = 0$. To avoid interactions between the polarized atoms the atomic beam intensity was always adjusted such that the surface coverage with ^{7}Li atoms never exceeded 10^{-3} of a monolayer. A variable magnetic field could be applied to the solenoidal magnet surrounding the sample surface. Because of the hyperfine interaction between the valence electron and the nucleus, the nuclear polarization of the incident atomic beam will change while the atoms are entering the magnetic field region over the surface; this essentially trivial effect is taken into account in analyzing the experimental data in order to extract the "true" magnetic field dependence of the depolarization rate.

The adsorbed ^{7}Li desorbs thermally from the surface partly as neutral atoms and partly as positive ions. The latter were extracted from the surface, accelerated, deflected by an electrostatic mirror, and analyzed by beam-foil spectroscopy to determine their first-rank or vector polarization P. (Since the Li ions are in an s state, there is no hyperfine interaction when the ions are extracted from the magnetic field region over the surface.) For a spin $I = {}^3/_2$ nucleus such as ^{7}Li, the vector polarization is defined by eq 13. As pointed out above, even though the time dependence of the polarization of the desorbing ^{7}Li ions consists, in general, of a sum of up to three exponential relaxation rates, for the choice of beam polarization and probe nucleus in the present case the nuclear spin relaxation as a function of time t can be described well by a single exponential with an effective temperature-dependent relaxation rate $\alpha(T)$, which is identical with the spin–lattice relaxation time T_1^{-1} in NMR experiments:

$$P(t) = P(0)\exp(-\alpha t) \quad (20)$$

Since for an adsorbed atom the probability to stay on the surface for a time t decreases exponentially as a function of (t/τ_R), where τ_R is the mean residence time, the temperature dependence of the polarization $P(T)$ of the desorbing ions is related to the effective relaxation rate α by eq 8.

In these experiments, the mean residence time τ_R was always measured separately for each given temperature by chopping the unpolarized atomic beam mechanically and measuring the decrease in beam-foil current of desorbing ions in the "afterglow" following the shutting off of the atomic beam. Thus, by measuring for a given temperature T the magnetic field dependent polarization $P(T,B)/P_0(B)$ and $\tau_R(T)$, the relaxation rate $\alpha(T,B)$ could be extracted.

Figure 14 displays in a semilogarithmic plot the effective relaxation rate α at $T = 1125$ K (residence time $\tau = 0.3715$ s) as a function of the external magnetic field strength B. The abscissa is displayed as a function of the Larmor frequency (top) as well (eq 2, for ^{7}Li $\omega_L = 1.03 \times 10^5\ s^{-1}\ B/mT$). There is no doubt that the data are not consistent with a magnetic-field-independent or frequency-independent relaxation rate as predicted in the low-frequency limit for three-dimensional diffusion. The solid line in Figure 14 represents a descrip-

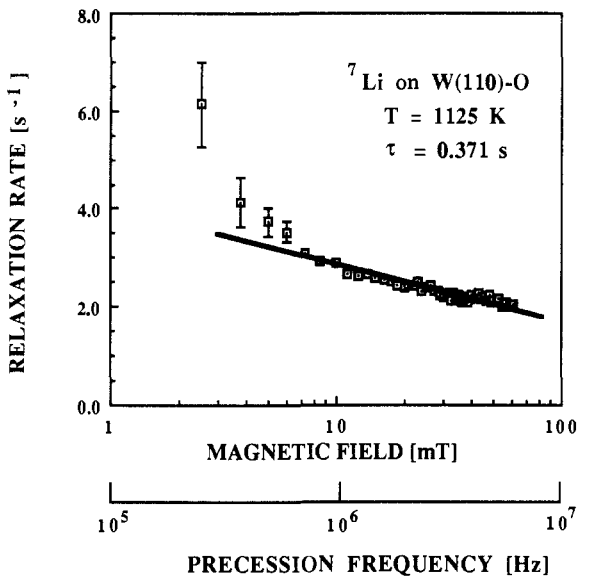

Figure 14. Experimentally measured values for the depolarization of ^{7}Li on an oxygen-covered W(110) surface as a function of the guide magnetic field. From ref 34.

tion of the data for $B > 7$ mT with a spectral density function appropriate to two-dimensional diffusion. Even though the data deviate from the description of two-dimensional diffusion for $B < 7$ mT, the magnetic field/frequency dependence of most of the data points bears out strongly the conjecture of a two-dimensional diffusion process.

Magnetic field dependences were also determined for several other surface temperatures between 1050 and 1200 K as well, and the data were analyzed as described above. The hopping times $\tau_c(T) = \tau_0 \exp(E_d/k_BT)$, with E_d as the diffusion energy, were then plotted as a function of the inverse temperature, $1/k_BT$. Even though the error bars are quite large and the data therefore scattered quite a bit, their trend generally was found to follow an Arrhenius curve with an assumed prefactor (typical phonon frequency) of $\tau_0 = 10^{-13}$ s and $E_d = 1.14$ eV. Due to the statistical fluctuations in the data these values are subject to a large uncertainty, but they agree reasonably well with values determined for similar systems in comparable experiments.[34,35]

This experiment thus establishes the general idea that depolarization is dominated by a two-dimensional process, probably surface diffusion, in the case of polarized alkali atoms on metal surfaces. The question remains, however, why one should have seen what appears to be a clearly defined trend away from the two-dimensional field at the lowest fields, 10 mT and less. The critical field for ^{7}Li is 28.7 mT, so the deviation comes about when the coupling to the field is significantly less than the hyperfine interaction energy. One possibility is that the surface magnetic field is no longer negligible at these low guide fields and that the nucleus is sensing the combined surface and applied fields. Further measurements of these effects are continuing.

VI. Future Directions in Nuclear Surface Physics

The foregoing experiments suggest a number of ways in which a generalized nuclear surface physics ansatz using nuclear-spin-polarized atomic beams can contribute to our understanding of surface chemical physics. This potential arises, on the one hand, from the inherently localized and nondestructive nature of the probe, and on the other from the availability of probe atoms with a significant range of nuclear dipole and quadrupole moments as well as a wide variety of chemical interactions with the sample surface. Thus surface physics experiments with polarized beams could have a significant impact on our understanding of phenomena ranging from surface magnetism to surface chemistry and diffusion dynamics. For example, calculations have shown that while alkalis tend to donate electrons to the surface and thus act as promoters, halides appear to draw electrons out of the surface and "poison" its chemical activity.[36,37] If it were possible to make beams of polarized chlorine, one could imagine experiments in which changes in surface chemical activity due to differing localized configurations of electronic charge could be studied in detail by comparing the depolarization rates of sodium and chlorine.

In evaluating the impact of nuclear-spin polarized atomic-beam techniques on surface spectroscopy, it is helpful to consider, in turn, the generic components of this type of experiment: (i) sources of spin-polarized nuclei; (ii) techniques for controlling the residence (interaction) time on (with) the surface; (iii) methods for measuring the nuclear polarization after the interaction; and (iv) spin-perturbation techniques which are applied to the nucleus on the surface. The initial experiments have set both a certain style and direction and also left clues to potential improvements and generalizations. If one attempts to evaluate the potential for future developments, it is evident that there are several limitations in present experiments that are in no way inherent in the technique.

To become a generally applicable tool in surface physics, each of these elements of the generic nuclear surface physics experiment needs to have certain features, which are readily enumerated. First, the source of spin-polarized nuclei should be capable of providing probes suitable for the exploration of diverse surface phenomena: catalysis or promotion, poisoning, diffusion, surface magnetism, and bonding, for example. Second, the method for controlling the residence time must be efficient, should not destroy the sample surface, and should work on essentially arbitrary surfaces at arbitrary temperatures. Third, the polarization measurement technique should allow for the detection of either ions or atoms with high efficiency so that required surface coverage by the polarized nuclei is minimal. Finally, it should be possible to borrow some of the sophisticated rf pulse techniques from more conventional NMR experiments to, for example, allow refocusing of spins and hence longer residence times. It appears that all of these conditions can, in principle, be satisfied in ways that are neither excessively costly nor unbearably complicated.

A. Potential Polarized Probe Nuclei

The alkali metals are certainly not the only ones presently producible in the classic *rf atomic beam source*. Hydrogen and deuterium atomic beam polarized sources, for example, have a long and honorable

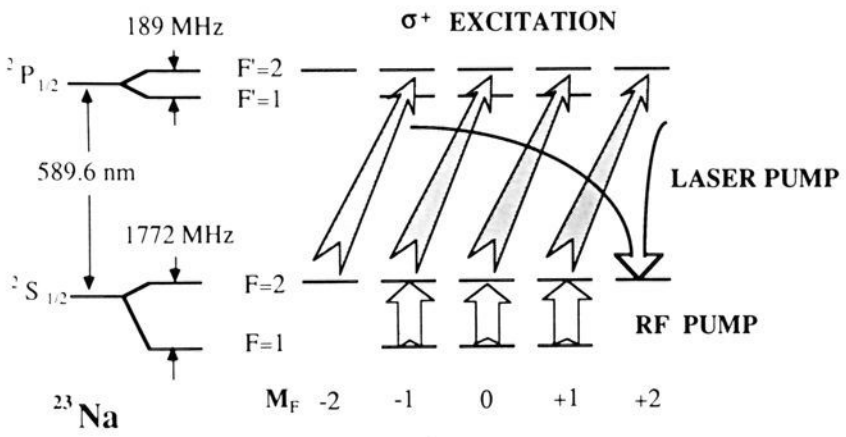

Figure 15. Optical pumping scheme for producing polarized alkalis by rf–optical double resonance.

history in low-energy nuclear physics.[7] A typical hydrogen/deuterium atomic beam source is similar to the polarized alkali source of Figure 3, except that the evaporation oven is replaced by a gas bottle and a dissociative rf discharge circuit. Some attempts have also been made to polarize both nitrogen and fluorine in an atomic beam source,[38] and it appears that there are no obstacles in principle to building working polarized sources for these species. Since submonolayer coverages are desirable for surface spectroscopy, the beam currents required for nuclear surface physics experiments are of order 10^{13} particles/s, some 3 orders of magnitude less than the typical required current for polarized-ion sources for accelerator applications.

A second interesting class of ion sources produces polarized nuclei by any of several *optical pumping* schemes.[39,40] The optical pumping technique can be chosen to preferentially populate a single state having a specific electronic and nuclear spin. In one such scheme—for producing a polarized sodium beam—both a tunable dye laser and a resonant rf cavity are deployed in a double-resonance configuration, illustrated schematically in Figure 15.[40] The relevant atomic energy levels, whose quantum numbers are conventionally denoted by total angular momentum F and magnetic quantum number m_F, are shown in the figure. Right circularly polarized light is used to pump from the $F = 2$ ground-state levels to the $F = 2$ levels of the first excited state of ^{23}Na. Since there is, in effect, no exit from $F = 2$, $m_F = 2$ state (which corresponds to nuclear spin $I = {}^3/_2$, $m_I = {}^3/_2$), all the atoms excited by the laser light eventually arrive at that state—except for those that undergo radiative decay to the $F = 1$ hyperfine levels of the ground state. These atoms, however, are continually being excited into the $F = 2$ hyperfine level of the ground state by the rf field applied at the hyperfine frequency. In a practical optically pumped atomic beam source, a thermal velocity beam of alkali atoms is produced in an oven and allowed to effuse through a collimator into an rf resonator, where circularly polarized D_1 radiation from a single-mode ring dye laser excites transitions between the ground state and first excited states of the atom. Transitions between the $F = 1$ and $F = 2$ hyperfine sublevels are induced simultaneously by an applied rf field at the hyperfine frequency (1.772 GHz for sodium, for example). If the laser pump frequency is chosen to match the $F = 2$ to $F' = 2$ transition, for example, the applied rf field serves to continually repump the $F = 2$ levels with atoms having hyperfine quantum number $F = 1$, thus maximizing the polarized beam current for a given source flux. The end result of this process is a beam with a population of approximately 0.95 in the state $F = 2$, $m_F = 2$.[40] Other magnetic sublevels m_F of the $F = 2$ ground-state hyperfine manifold can be populated by the addition of an adiabatic rf transition with a static magnetic field gradient.

Similar principles can be applied to many other kinds of atomic systems, making this a particularly versatile source of polarized beams. Other nuclei that have been polarized by optical pumping include ^3He, in this case by using flash lamp pumped tunable dye lasers to produce light at 1.08 μm.[41] Optical pumping is also an effective technique for producing nuclear orientation in short-lived radionuclides at the output of a mass separator.[42] As has been pointed out by Fick,[43] short-lived β-emitting polarized nuclei could be used to measure the time histories of depolarizing interactions on cold surfaces using well-known nuclear detection techniques.

A third class of ion sources having broad potential applicability is the *spin-transfer* source. In these sources, electron-spin-polarized atoms—produced, for example, by optical pumping or in a multipole separation magnet—are allowed to interact with the atoms that are to be polarized, and the contact interaction (hyperfine interaction) between the nuclei gradually transfers electronic polarization to the nucleus.[44] This interaction may take place either between crossed beams[45] or in a container that encloses both the polarized and the polarizable species in a volume with relatively inert walls. Large polarizations have been produced both in thermal velocity odd-A noble gas isotopes and in fast proton beams[46] by this technique, and in principle it should be possible to produce polarized atomic beams of many other elements in this way. The concept of a "polarized beam in a bottle" is particularly of interest in surface physics applications, because the number density of polarized atoms now produced in several experiments (of order 10^{17} atoms/cm^3, with polarizations ranging up to a few tens of a percent[44]) is sufficient to provide a particle current equal to that of a compact atomic beam source for many hours. Implementation of this concept requires entraining the polarized nuclei—say, in a jet of a noble carrier gas—to provide transport to the target. However, the requisite transport distances are so short that even a beam with poor emittance characteristics would probably be sufficient.

It is instructive to group the presently available polarized atomic species according to their known chemical interactions with surfaces, as in Table II. From these few examples, it is clear that were one to develop polarized sources in which the probe species could be changed by simply inserting a new gas or metal source, a variety of chemical physics experiments comparing the electronic charge distributions in contrasting chemical situations could be carried out. One nucleus that does not appear on this list is ^{13}C—one whose significance to the chemical and biological research communities is hard to overestimate. While ^{13}C beams are produced in accelerators, there have apparently been no attempts to produce polarized ^{13}C nuclei thus far. This may be partly because of the difficulty of polarizing any species that does not have an unpaired electron, since most nuclear polarization techniques rely

TABLE II. Polarized Source Types with Potential Surface Applications

nucleus	spin	μ/μ_B	Q, mb	polarization scheme	applications
^{1}H	$^{1}/_{2}$	2.793		atomic beam	blocking, bonding, surface diffusion
^{2}D	1	0.857	2.74	optical pumping	
^{3}T	$^{1}/_{2}$	2.979		spin transfer	
^{6}Li	1	−0.82	−0.8	atomic beam	promoting (catalysis)
^{7}Li	$^{3}/_{2}$	−3.256	−37.6	optical pumping	
^{23}Na	$^{3}/_{2}$	−2.217	110.0		
^{8}Li	(2)	1.653		mass separator with optical pumping	promoting (catalysis)
^{14}N	1	0.404	16.0	atomic beam	blocking, bonding, catalysis
^{19}F	$^{1}/_{2}$	2.627		atomic beam	surface poisoning
^{35}Cl	$^{3}/_{2}$	0.821	−79.0		
^{3}He	$^{1}/_{2}$	−2.127		optical pumping	surface magnetism, diffusion
^{21}Ne	$^{3}/_{2}$	−0.662	90.0	spin transfer	
^{89}Kr	$^{9}/_{2}$	−0.967	220.0		
^{131}Xe	$^{3}/_{2}$	0.691	−120.0		

on using the unpaired electron to transfer polarization in some way to the nucleus.

B. Arbitrary Control of Residence Time

In present experiments, the residence time of the polarized adsorbed nuclei is adjusted by changing the temperature of the surface. This has some serious disadvantages in addition to the obvious one that many worthy objects of study—both phenomena and materials—may not occur in a temperature range where the desired yield and polarization of the desorbing nuclei are physically possible. First, at elevated temperatures, the adsorbed atoms diffuse about on the surface, making it impossible to study *local* (as contrasted with averaged) potentials. Second, some adsorbed species—the classic example is hydrogen—desorb thermally as molecules rather than as atoms. Third, it may be difficult or even impossible in many cases to carry out NMR measurements at elevated temperatures because of the conflicting needs to have a sufficiently large polarization to see a signal while at the same time allowing the nucleus to stay long enough in the perturbing field that the measured transition is fully saturated. Hence it is important to have at hand some type of desorption technique that allows one to retain arbitrary control of the residence (interaction) time of the polarized nuclei on the surface.

Stimulated desorption by electrons, photon beams, or laser beams appears to be one promising avenue of approach. In electron-stimulated desorption (ESD) experiments, for example, beams of electrons of energy of up to a few hundred electronvolts have been successfully used to desorb copious quantities of neutral hydrogen atoms from alkali halide surfaces. The ESD process for adsorbed atoms is still not completely understood; indeed, the mechanisms whereby neutral ground-state and excited-state atoms are efficiently produced in ESD even on simple materials such as alkali halides is still a subject of active investigation.[48] For our present purposes, however, three features of ESD deserve particular mention: ESD occurs on a time scale ($\approx 10^{-13}$ s) that is exceedingly short compared to the Larmor frequencies of the alkalis and of hydrogen; ESD apparently produces excited-state atom desorption in a direct surface process;[49] and ESD can be carried out in regimes where relatively little damage is done to sample surfaces during the irradiation. Hence, it appears that ESD can be used to control residence time at least for polarized adatoms on semiconductors, and probably on insulators as well. It is not yet clear to what extent ESD can be used to recover adsorbed atoms from metallic surfaces; further experiments will be required to ascertain whether yields are sufficient at low coverages to permit accurate polarization measurements.

Photon-stimulated desorption (PSD) using *laser* photons may represent an eminently practical solution to the control of residence time, particularly for alkalis adsorbed on metallic or semiconductor crystal surfaces, since the laser pulse induces desorption by strong but highly localized heating of the substrate. While the precise interplay of thermal and nonthermal desorption mechanisms is still not well understood,[50,51] the primary desorption mechanism, at least at visible and infrared wavelengths, appears to be thermal ejection of adsorbates arising from rapid heating of the surface during the laser pulse (typically a few nanoseconds). For polarized species that can be desorbed thermally (e.g., the alkalis), the use of a laser pulse to which the detection electronics can easily be synchronized with subnanosecond jitter is very likely to be advantageous; this capability would be especially important, for example, in the application of pulsed NMR techniques. Again, because of the short duration of the laser pulse, the desorption time is still rapid compared to the characteristic time scales of the nuclear spin precession.

Regardless of the technique chosen, it is clear at this point that freeing the experiments from the somewhat arbitrary requirements of thermal desorption will have a large effect on the variety and sophistication of experiments that can be carried out.

C. Nuclear Polarization Measurements on Desorbing Neutral Atoms

The beam-foil monitoring technique is clearly useful for polarization measurements on desorbing ion species and has the inestimable advantages of simplicity, inexpensive realization in practice, and ease of operation. However, beam-foil polarization monitoring can only be effective in studies of surfaces that have work functions not too different from the ionization energies of the adsorbed species. Hence, it is a technique that works well for alkalis on metals and even some semiconductors, but not much else. Moreover, since different index faces of even the same substrate material may exhibit substantial variations in work functions, it is inconvenient to rely on this type of polarization measurement for wide-ranging or systematic studies.

One effective technique now successfully demonstrated in the context of nuclear surface physics is for

polarization detection is laser-induced fluorescence (LIF) in a magnetic field.[25,52,53] A small fraction of the atoms in each Zeeman level is excited by the laser light as the laser is tuned through the resonance line, and the fluorescence from the decays to the ground state is monitored with a photodetector. The laser is highly efficient at producing fluorescence; a sample of only some 10^8 atoms in the focal volume of the laser can be seen in this way. Moreover, unlike the beam-foil technique, which measures the product of polarization and analyzing powers, LIF gives a direct measure of the relative magnetic substate population and hence provides information on all ranks of polarization with equal sensitivity. In beam-foil spectroscopy, one the other hand, all the measured polarizations are weighted by the corresponding analyzing powers—and, as is the case with third-rank analyzing powers, a small or vanishing analyzing power for a particular ion species means that there is no sensitivity to the corresponding polarization t_{kq}. With LIF detection, one also has in many cases the option of pumping at one wavelength and detecting at another wavelength to reduce background signals. This can be done, as has already been pointed out in an earlier review, for polarized hydrogen atoms desorbed by electron impact, since the excited hydrogen atoms desorb to a large extent in the metastable 2s state; hence, it would be possible to pump the visible 2s–3p transition with a tunable dye laser and monitor the ultraviolet transition back to the ground state.[54] In such cases, not only is the signal-to-noise ratio enhanced by filtering out the optical pumping signal, but there may be a more favorable branching ratio into the detected transition, so that the absolute yield is also increased.

Another laser-based technique for monitoring the polarization is the use of pulsed lasers to do resonant multiphoton ionization (RMPI) of the desired desorbing neutral species, followed by detection of the ions in a channeltron detector.[55,56] This technique has the advantage over LIF in its nearly universal applicability, and for many experimental geometries can be even more efficient. In particular, for studies of ground-state, desorbed, polarized hydrogen, it is probably the only possible technique.

D. Spin Perturbation Techniques

Up to now, NMR experiments with polarized beams have used continuous rf irradiation of the polarized nuclei on the surface to provide the perturbing field; for the continuous deposition and thermal desorption of polarized nuclei characteristic of the present experiments, this is clearly appropriate. However, the much more sophisticated rf pulse techniques now routinely employed in chemical and biological NMR studies would appear to be extremely useful, particularly on cold surfaces where nuclei would be allowed to remain for very long residence times. For example, appropriate multiple-pulse sequences can have the effect of averaging out rapid, isotropic motion, or even of "refocusing" nuclear spins that have become dephased through environmental interactions.[57] The use of two-dimensional NMR techniques and pulse sequencing would be critical to the success of polarized-beam experiments with adsorbed molecular species creating multiple electromagnetic environments for the adsorbed polarized nucleus as well.

One can conceive of taking advantage of the enormous body of NMR techniques in another way: by creating a hybrid technique, in which a polarized beam would be used to create a dense sample of probe nuclei on a surface, which would in turn be put into a standard NMR spectrometer and studied in the usual way. Preliminary calculations[58] suggest that the extractable signals may still be too small, even with modern NMR signal-processing techniques; however, the possibilities are so intriguing that the matter probably deserves a more rigorous analysis.

VII. Comments and Conclusions

The importance of spin-polarized surface probes has grown dramatically in recent years, particularly in explorations of surface magnetism.[59,60] Because of the state-specific character of polarization measurements with prepared probes—as in spin-polarized LEED and electron-spin-polarized metastable atom spectroscopy—polarization measurements offer a qualitatively superior access to detailed information about surface phenomena. As interest in surface science continues to shift to detailed studies of surface *dynamics*—in contrast to the historically earlier emphases on surface structure and surface composition—it seems only reasonable to suggest that polarization measurements will have an increasing impact.

Viewed within this context, the development of nuclear surface physics with polarized beams from a relatively specialized, even arcane mixture of nuclear, atomic, and surface physics into a truly general surface spectroscopy is likely to be of great significance. Because spin-polarized nuclei have both dipole and quadrupole moments and because of the great variety of available dipole-to-quadrupole ratios (Table II), the technique is inherently broad gauge in its application. Moreover, the fact that the technique can be used to obtain meaningful information on polycrystalline and amorphous surfaces, as well as single-crystal samples, augurs well for its practical applicability. The early restriction to the study of desorbing *ions* has already been removed by the use of laser-induced fluorescence to detect desorbing *atoms*; the introduction of resonant multiphoton ionization spectroscopy would add an even greater dimension in sensitivity. The control of residence time via thermal desorption can be broadened to include electron- or laser-stimulated desorption—thus permitting the study of a wider class of surfaces and adsorbates under virtually arbitrary temperature conditions. In addition, the substantial variety in the available polarized probe species will allow the use of probes suited to a wide variety of both fundamental and applied surface science problems. Thus, on the experimental side, there appears to be few obstacles to the use of SPNSS as a versatile and flexible technique for surface studies, providing unique information on surface electronic charge distributions complementary to that obtained from existing analytical techniques.

Increasing theoretical interest in the meaning of nuclear surface physics measurements is being stimulated by the awareness that this technique provides information complementary to tunneling microscopy, desorption spectroscopy, and other analytical techniques that probe surface electronic structure. However, there is a significant challenge to standard calculations, such

as fully self-consistent thin-film or slab calculations done on metal[61] and semiconductor[62] surfaces; computational limitations for these cases require the assumption of uniform adsorbate coverage over a relatively small unit cell. A recent comparison of average EFGs measured in NMR experiments on tungsten with theoretical values calculated from a model based on a jellium substrate with a single alkali adatom show some remarkable agreements, but systematic trends are not entirely consistent.[63] Further progress in dealing with structured substrates and with the more complex substrate electron distributions may well come from cluster-model calculations[64]—provided they can be improved so that the substrate parameters are calculated in a more nearly self-consistent manner. Additional insight—particularly into the dynamics of the spin-polarized probe on the surface—is also likely to come from increasingly powerful and well-articulated theories of gas–surface interactions.[65]

Theoretical studies of gas–surface interactions, in fact, are likely to point up some of the weaknesses or potential difficulties in the application of polarized-beam techniques to problems in surface chemical physics. Recent work in this area suggests, for example, that electronic states may be selectively populated in charge-exchange interactions at surfaces in ways that will lead to electron polarizations that could be transferred to the atomic nucleus via the hyperfine interaction.[66] Such a desorption- or charge-exchange-induced polarization would be interesting in its own right, of course; but, were that to occur, it would also require detailed understanding in order to separate the effects due to the residence time on the surface. In a related set of developments, traditional nuclear *solid-state* physics techniques, such as β-emitting implanted radionuclide spectroscopy[67] and muon spin rotation,[68] are, in amanner of speaking, working their way toward the surface and providing new and interesting insights into the selvedge where the bulk is transformed into a surface.

In summary, it appears that nuclear surface physics with polarized beams offers the promise of many new insights into studies both of surface structure and of surface dynamics. The technique, in a general way, is a natural extension of both nuclear and atomic physics techniques for the investigation of surfaces, and current experiments give every indication of developing interesting connections to standard nuclear magnetic resonance analysis. Prospects for the immediate future will revolve around a sorting out of the manifold possibilities of the technique and its application beyond the present narrow confines of polarized alkali nuclei on hot transition-metal surfaces.

VIII. Acknowledgments

The support of the North Atlantic Treaty Organization, through a grant of travel funds, for a collaborative with the research group of Professor D. Fick, Philipps-Universität, Marburg, Federal Republic of Germany, on this work is gratefully acknowledged. Related research at Vanderbilt University on desorption induced by electronic transitions, surface dynamics, and the effects of adsorbed overlayers is supported by the Air Force Office of Scientific Research and the Office of Naval Research.

IX. Mathematical Appendix: Polarization Formalism

1. Nuclear Multipole Moments and Electromagnetic Fields

The relationships between the Cartesian and spherical tensor forms of the dipole and quadrupole fields and nuclear moment operators are derived in numerous textbooks and are summarized here for convenience. The dipole terms in V_{1q} and M_{1-q} are

$$V_{1\pm1} = \pm\frac{1}{2}(B_x \pm iB_y) \qquad M_{1\pm1} = \pm\frac{1}{2^{1/2}I}\mu I_\pm \tag{A.1a}$$

$$V_{10} = B_z\, M_{10} = \pm\frac{I_z}{I} \tag{A.1b}$$

where the B_i are the Cartesian components of the surface magnetic field and I, $I_\pm$, and I_z are the conventional nuclear spin operators. The second-rank (quadrupole) fields V_{2q} interact with the second-rank nuclear moments M_{2q}, which are proportional to the nuclear quadrupole moment $e{\cdot}Q$:

$$V_{2\pm2} = \frac{1}{2(6^{1/2})}(V_{xx} - V_{yy} \pm 2iV_{xy})$$
$$M_{2\pm2} = \left[\frac{6^{1/2}}{4I(2I-1)}\right](e{\cdot}Q)I_+^2 \tag{A.2a}$$

$$V_{2\pm1} = \frac{1}{(6^{1/2})}(V_{xz} \pm iV_{yz})$$
$$M_{2\pm1} = \left[\frac{6^{1/2}}{4I(2I-1)}\right](e{\cdot}Q)(I_zI_\pm - I_\pm I_z) \tag{A.2b}$$

$$V_{20} = \frac{1}{2}V_{zz}$$
$$M_{20} = \left[\frac{1}{2I(2I-1)}\right](e{\cdot}Q)(3I_z^2 - I(I+1)) \tag{A.2c}$$

where the quantities V_{ij} are the electric field gradients in Cartesian coordinates and the $I_\pm$ are the angular momentum raising the lowering operators. It is to be emphasized that the V_{kq} are functions of the time and may comprise both a fluctuating component and a component that is slowly varying on the time scale of the nuclear Larmor precession $1/\omega_L$.

2. Nuclear Polarizations and Occupation Numbers

The elements of the density matrix are related to the spherical polarization tensors t_{kq} by the equation[12]

$$t_{kq} = \sqrt{(2I+1)}\sqrt{(2k+1)}\sum_{mm'}(-1)^{I-m-q}(IIk|m-m'q)\rho_{mm'}{}^I \tag{A.3}$$

where the quantity in parentheses is a Wigner 3-J coefficient. The range of the index k is from 0 to $2I$; the subscript q, in turn, varies from $-k$ to $+k$. The spherical tensors t_{kq} are related to the Cartesian tensors P_{ijk} (assuming the coordinate system of Figure 2) as follows:

spin-1 nuclei

$$t_{10} = \left(\frac{3}{2}\right)^{1/2}(N_1 - N_{-1}) = \left(\frac{3}{2}\right)^{1/2}P_z \quad \text{(A.4a)}$$

$$t_{20} = \left(\frac{1}{2}\right)^{1/2}(N_1 - 2N_0 + N_{-1}) = \left(\frac{1}{2}\right)^{1/2}P_{zz} \quad \text{(A.4b)}$$

spin-3/2 nuclei

$$t_{10} = \left(\frac{9}{5}\right)^{1/2}\left[N_{+3/2} - N_{-3/2} + \frac{1}{3}(N_{+1/2} - N_{-1/2})\right] = \left(\frac{9}{5}\right)^{1/2}P_z \quad \text{(A.5a)}$$

$$t_{20} = N_{+3/2} + N_{-3/2} - N_{+1/2} - N_{-1/2} = P_{zz} \quad \text{(A.5b)}$$

$$t_{30} = \left(\frac{9}{5}\right)^{1/2}\left[\frac{1}{3}(N_{+3/2} - N_{-3/2}) - (N_{+1/2} - N_{-1/2})\right] = \left(\frac{9}{5}\right)^{1/2}P_{zzz} \quad \text{(A.5c)}$$

In the vernacular of the nuclear polarization trade, the first-rank spherical (or Cartesian) tensor is referred to as the "vector polarization", while the second-rank spherical (or Cartesian) tensor is called the "tensor polarization". Clearly, of course, there is no consistent usage that distinguishes tensor polarization of the second and third ranks.

3. Derivation of the Transition Probabilities in Terms of the Hamiltonian

The equation of motion for the density matrix element $\rho_{mm'}$ is[12]

$$\frac{\partial\rho_{m'm}}{\partial t} = i\omega_{mm'}\rho_{m'm}(t) - \frac{2\pi i}{h}\langle Im'|[V_{kq}(t),\rho(t)]|Im\rangle + \sum_{n,n'}R_{m'mn'n}\rho_{n'n}(t) \quad \text{(A.6)}$$

where the first term contains the trivial harmonic variation of the unperturbed spin system, the second term containing the commutator of $V_{kq}(t)$ with the density matrix ρ represents the "static" (i.e., slowly varying on the time scale of the Larmor frequency) interactions of the nucleus with external perturbing fields, and the last term represents the irreversible interaction of the nucleus with the undetected reservoir of surface atoms R. The summation extends over the repeated indices n and n'.

In experiments starting with a beam whose nuclear substate populations are well defined by the properties of the source, it is reasonable to assume that the relaxation term involves only diagonal elements of the density matrix. It is also convenient and appropriate to assume that the interaction between the spin system S and the reservoir R has the separable form

$$U_{SR} = \sum_{i,j}U_iF_j \quad \text{(A.7)}$$

where the U_i act only on the variables of the spin system S and the F_j act only on the reservoir. Under these two assumptions, the relaxation term $R_{m'mn'n}$ turns out to have the particularly simple form

$$R_{nmmn} = \frac{4\pi^2}{h^2}\sum_{ij}\langle n|U_i|m\rangle\langle m|U_j|n\rangle\int_0^\tau dt' \langle F_i(t-t')\cdot F_j(t)\rangle \exp(-i\omega_{mn}t') \quad \text{(A.8)}$$

where the brackets indicate averages taken over the reservoir or the spin system as appropriate and the integral extends over the interaction time τ. For the diagonal elements of the density matrix, the relaxation term in fact has the form of a transition probability W_{mn} between states m and n.

We now introduce the two key assumptions needed to evaluate the W_{mn}. The first is that the reservoir R has so many degrees of freedom that all interactions with the spin system S are dissipated so quickly that R remains in a thermal equilibrium distribution, irrespective of changes in S. The second is that the time derivative of the density matrix depends only on its present value, and that the reservoir therefore has no memory of its interactions with the spin system S beyond some typical time interval that is conventionally called the *correlation time* τ_c. (In statistical terminology, this is the Markoff approximation.) Under this assumption, it follows that the expectation values $\langle F_i(t-t')\cdot F_j(t)\rangle$ (which in fact express the time correlation behavior of the interaction between the spin system and the reservoir) vanish for time differences greater than τ_c, so that it is permissible to replace the upper limit of the integral in eq A.8 by ∞. Then the integral over the reservoir interactions becomes

$$R_{nmmn} = \int_0^\infty dt' \langle F_i(t-t')\cdot F_j(t)\rangle \exp(-i\omega_{mn}\tau) = \int_0^\infty dt' G_{ij}(t-t') \exp(-i\omega_{mn}t') \quad \text{(A.9)}$$

which has the standard form of *spectral density functions* giving the strength of the relaxing interaction as a function of frequency. The quantity in brackets in the first integral is the correlation function of $F(t)$ and is identified in the conventional way in the second integral. Note that the subscripts ij indicate the relevant quantum numbers for the spin–reservoir interaction and hence will reflect the kq of the nuclear polarization when we substitute the real potential terms. To avoid confusion with the V_{kq} introduced for the static fields, we shall denote the *fluctuating* part of the spin-interaction potential as U_{kq}, and, by using the Wigner–Eckhart theorem to write the fluctuating parts of the Hamiltonian as a direct product of electromagnetic field components and nuclear multipole moments, we obtain

$$W_{mm'} = \sum_{kk'}J_{kk'}(\omega_{mm'})|U^*_{k-q}|\cdot |U_{k'q}|(IIk|m\text{-}m'q)(IIk'|m\text{-}m'q')\cdot\langle I\|M_k\|I\rangle\langle I\|M_{k'}\|I\rangle \quad \text{(A.10)}$$

The quantities of interest for surface spin relaxation studies are the mean-square fluctuating multipole fields on the surface, since these can be directly related to electronic charge distributions experienced by the diffusing nucleus. The reduced matrix elements are of course known once the probe nucleus is chosen.

However, what is not known a priori is the form of the spectral density function $J(\omega_{m'm})$; it must be guessed from reasonable assumptions about the form of the correlation function. Each different assumption about the correlation function involves a different set of

physical possibilities. Much work has been done in this area in recent years because of studies of polarized quantum liquids, such as ^{3}He, on surfaces—where many studies of NMR have been carried out. As has been pointed out by Scholl,[31] the frequently assumed Bloembergen–Pound–Purcell (BPP) form of the correlation function predicts the wrong form for the spectral density functions compared to many experiments. For the physical situation realized in current nuclear surface physics experiments, the correlation function has been assumed to have the simple exponential form

$$G(\tau) = G(0) \exp(-\tau/\tau_c) \qquad \text{(A.11)}$$

where τ_c, the *correlation time*, is the characteristic time beyond which the memory of the depolarizing interaction between reservoir and spin system is lost. On a hot surface, the correlation time is the inverse of the jumping rate Γ, which is considerably shorter than the inverse of the transition frequency between eigenstates of the unperturbed Hamiltonian, $\omega_{mm'}$. Hence in this case—the instance of "extreme motional narrowing"—the denominator approaches unity and the correlation function reduces to the constant $2\tau_c$. Under these assumptions, the correct form of the spectral density function for all dimensions has been derived by several authors.[31-33]

Thus, under the conditions of (1) high surface temperatures (motional narrowing), (2) a Markovian relaxation process, and (3) no interaction among the polarized probe nuclei, we have to deal with only two extreme types of interactions between the polarized nuclei and the surface that can be studied by the experimental techniques to be described below. We note that in NSR experiments, the depolarization mechanism is the randomly fluctuating electromagnetic fields and field gradients experienced by the nucleus as it diffuses about on the surface. The time scale of the interactions is so short that the nuclear depolarization comes from the myriad small perturbations it experiences before being desorbed. In NLM and NMR experiments, the residence time is so short that depolarization is dominated by the externally imposed fields, whose time variation is slow compared to the characteristic spin precession frequencies of the polarized nucleus. The density-matrix formalism encompasses both of these regimes, as well as the problematical regime of interaction times in between these extremes.

On the other hand, on cold surfaces this simple approximation no longer holds, especially in the region for which $\tau_c \approx 1/\omega_{mm'}$. There the competition between the jumping rate and the Larmor frequency changes the physics to the point where the simplifying approximations made possible by motional narrowing no longer hold. Moreover, the assumption that only the diagonal terms of the relaxation tensor R_{mmmn} contribute to the magnetic substate populations cannot be true in general.

X. References

(1) Among the crucial "founders' papers" are those by: Bloch, F.; Hansen, W. W.; Packard, M. *Phys. Rev.* **1946**, *69*, 127. Purcell, E. M.; Torrey, H. C.; Pound, R. V. *Phys. Rev.* **1946**, *69*, 37. Bloch, F. *Phys. Rev.* **1946**, *70*, 460. Bloembergen, N.; Purcell, E. M.; Pound, R. V. *Phys. Rev.* **1948**, *73*, 679. The evolution of nuclear magnetic resonance analysis in chemistry is traced by: Jonas, J.; Gutowsky, H. S. *Annu. Rev. Phys. Chem.* **1980**, *31*, 1.

(2) Reviews of surface magnetic resonance studies with special emphasis on systems relevant to catalysis are those by Slichter (Slichter, C. P. *Annu. Rev. Phys. Chem.* **1986**, *37*, 25) and the earlier work by Duncan and Dybowski (Duncan, T. M.; Dybowski, C. *Surf. Sci. Rep.* **1981**, *1*, 157).

(3) General considerations relevant to nuclear magnetic resonance studies of adsorbed molecular complexes are discussed in the review by: Pfeifer, H.; Meiler, W.; Deininger, D. *Annu. Rep. NMR Spectrosc.* **1983**, *15*, 291.

(4) Horn, B.; Dreves, W.; Fick, D. *Z. Phys. B: Condens. Matter* **1982**, *48*, 335.

(5) Holm, U.; Steffens, E.; Albrecht, H.; Ebinghaus, H.; Neuert, H. *Z. Phys.* **1970**, *233*, 415. Also: Steffens, E.; Ebinghaus, H.; Fiedler, F.; Bethge, K.; Engelhardt, G.; Schafer, R.; Weiss, W.; Fick, D.; *Nucl. Instrum. Methods* **1975**, *124*, 601.

(6) Steffens, E.; Dreves, W.; Ebinghaus, H.; Kohne, M.; Fiedler, F.; Egelhof, P.; Engelhardt, G.; Kassen, D.; Schafer, R.; Weiss, W.; Fick, D. *Nucl. Instrum. Methods* **1977**, *143*, 409.

(7) Haeberli, W. *Annu. Rev. Nucl. Sci.* **1967**, *7*, 373.

(8) Böttger, R.; Egelhof, P.; Möbius, K.-H.; Presinger, D.; Steffens, E.; Dreves, W.; Horn, B.; Koenig, I.; Fick, D. *Z. Phys. A* **1981**, *299*, 291.

(9) Abragam, A. *The Principles of Nuclear Magnetism*; Oxford University: Oxford, 1961; pp 145, 163.

(10) Slichter, C. P. *Principles of Magnetic Resonance*, 2nd ed.; Springer-Verlag: Berlin, 1980; pp 141, 158–167.

(11) Simonius, M. In *Lecture Notes in Physics*; Fick, D., Ed.; Springer-Verlag: Berlin, 1980; Vol. 30, pp 38–113.

(12) Blum, K. *Density Matrix Theory and Applications*; Plenum: New York, 1981.

(13) Memmert, U. Ph.D. Dissertation, Philipps-Universität, Marburg, FRG, 1987.

(14) Andrä, H.-J.; Plöhn, H. J.; Gaupp, A.; Fröhling, R. *Z. Phys. A* **1977**, *281*, 15.

(15) Murnick, D. E.; Feld, M. S. *Annu. Rev. Nucl. Part. Sci.* **1979**, *29*, 411.

(16) Memmert, U.; Fick, D. *J. Phys. E: Sci. Instrum.* **1988**, *21*, 208. Dreves, W.; Jänsch, H.; Koch, E.; Fick, D. *Phys. Rev. Lett.* **1983**, *50*, 1759.

(17) Beckmann, E. Ph.D. Dissertation, Philipps-Universität, Marburg, FRG, 1984.

(18) See, for example: DiFoggio, R.; Gomer, R. *Phys. Rev. B: Condens. Matter* **1982**, *25*, 3490.

(19) Fick, D.; Haglund, R. F., Jr.; Beckmann, E.; Horn, B.; Koch, E. *Nucl. Instrum. Methods Phys. Res., Sect. B* **1984**, *B2*, 360.

(20) Beckmann, E.; Horn, B.; Fick, D. *Surf. Sci.* **1984**, *147*, 263.

(21) Koch, E.; Horn, B.; Fick, D. *Phys. Lett. A* **1985**, *109A*, 355.

(22) Fick, D.; Haglund, R. F., Jr.; Tolk, N. H. *Proceedings International Workshop on Desorption Induced by Electronic Transitions (DIET-II), Elmau, 1984*; Menzel, D., Brenig, W., Eds.; Springer-Verlag: Heidelberg, 1985; p 216.

(23) Horn, B.; Koch, E.; Fick, D. *Phys. Rev. Lett.* **1984**, *53*, 364.

(24) Koch, E.; Horn, B.; Fick, D. *Surf. Sci.* **1986**, *173*, 639.

(25) Memmert, U.; Fick, D. *Europhys. Lett.* **1988**, *5*, 185. Memmert, U.; Fick, D. *Surf. Sci.*, in press.

(26) Wassmuth, K.; Fick, D. *Phys. Rev. Lett.* **1987**, *59*, 3007. Also, Wassmuth, K.; Fick, D. *Nucl. Instrum. Meth. Phys. Res.* **1988**, *A267*, 22.

(27) Langmuir, I. *J. Am. Chem. Soc.* **1932**, *54*, 2798.

(28) Gurney, R. W. *Phys. Rev.* **1935**, *47*, 479.

(29) Doll, J. D.; Voter, A. F. *Annu. Rev. Phys. Chem.* **1987**, *38*, 413.

(30) Naumovets, A. G.; Vedula, Yu. S. *Surf. Sci. Rep.* **1984**, *4*, 365.

(31) Scholl, C. A. *J. Phys. C* **1981**, *14*, 447.

(32) Cowan, B. P. *J. Low Temp. Phys.* **1983**, *50*, 135.

(33) Avagadro, A.; Villa, M. *J. Chem. Phys.* **1977**, *66*, 2359. Bjorkstam, J. L.; Villa, M. *Phys. Rev. B: Condens. Matter* **1980**, *B22*, 5025.

(34) Memmert, U.; Bickert, M.; Riehl, M.; Wassmuth, K.; Fick, D.; Haglund, R. F., submitted for publication in *Hyperfine Interact.*

(35) Ehrlich, G.; Stolt, K. *Annu. Rev. Phys. Chem.* **1980**, *31*, 603.

(36) Lang, N. D. *Commun. Solid State Phys.* **1978**, *8*, 147.

(37) Feibelman, P. J.; Hamann, D. R. *Phys. Rev. Lett.* **1984**, *52*, 61.

(38) Dunham, J. S.; Galovich, C. S.; Wissink, S. W.; Mavis, D. G.; Hanna, S. S. In *Polarization Phenomena in Nuclear Physics—1980*; AIP Conf. Proc. No. 69; Ohlsen, G. G., et al., Eds.; American Institute of Physics: New York, 1981; pp 941–943.

(39) Murnick, D. E.; Feld, M. S. *Annu. Rev. Nucl. Part. Sci.* **1979**, *29*, 411.

(40) Dreves, W.; Jänsch, H.; Koch, E.; Fick, D. *Phys. Rev. Lett.* **1983**, *50*, 1759. Detailed descriptions of a working source, including extensive design discussions, will be found in: Bechtel, H. Dissertation, Philipps-Universität, Marburg, FRG, 1985, unpublished.

(41) Slobodrian, R. J. In *Polarization Phenomena in Nuclear Physics—1980*; AIP Conf. Proc. No. 69; Ohlsen, G. G., et al., Eds.; American Institute of Physics: New York, 1981; pp 797–802.

(42) For examples of recent work in this area, see: Lasers in Nuclear Physics; Bemis, C. E., Carter, H. K. Eds.; Harwood: Chur, Switzerland, 1982.
(43) Fick, D. Proceedings of the 6th International Symposium on Polarization Phenomena in Nuclear Physics, *J. Phys. Soc. Jpn.* **1986**, *55*, 423. Fick, D.; Horn, B.; Koch, E.; Memmert, U. *Z. Naturforsch.* **1986**, *41a*, 113.
(44) Happer, W.; Miron, E.; Schaefer, S.; Schreiber, D.; van Wijngaarden, W. A.; Zeng, X. *Phys. Rev. A* **1984**, *29*, 3092.
(45) Anderson, L. W.; Kaplan, S. N.; Pyle, R. V.; Ruby, L.; Schlachter, A. S.; Stearns, J. W. *Phys. Rev. Lett.* **1984**, *52*, 609.
(46) Bhaskar, N. D.; Happer, W.; McClelland, T. *Phys. Rev. Lett.* **1982**, *49*, 25.
(47) Witteveen, G. J. *Nucl. Instrum. Methods* **1979**, *158*, 57.
(48) Haglund, R. F., Jr.; Albridge, R. G.; Cherry, D. W.; Cole, R. K.; Mendenhall, M. H.; Peatman, W. C. B.; Tolk, N. H.; Niles, D.; Margaritondo, G.; Stoffel, N. G.; Taglauer, E. *Nucl. Instrum. Methods Phys. Res.* **1986**, *B13*, 525.
(49) Haglund, R. F.; Albridge, R. G.; Barnes, A. V.; Mendenhall, M. H.; Tolk, N. H.; Ramaker, D. A., to be submitted to *Phys. Rev. B*.
(50) Chuang, T. J. *Surf. Sci. Rep.* **1983**, *3*, 1.
(51) Rothenberg, J. E.; Kelly, R. *Nucl. Instrum. Methods Phys. Res. Sect. B* **1984**, *B1*, 291.
(52) Pappas, P. G.; Burns, M. M.; Hinshelwood, D. D.; Feld, M. S.; Murnick, D. E. *Phys. Rev. A* **1980**, *21*, 1955–1968.
(53) Jänsch, H.; Koch, E.; Dreves, W.; Fick, D. *J. Phys. D* **1984**, *17*, 231.
(54) Haglund, R. F.; Fick, D.; Horn, B.; Koch, E. *Hyperfine Interact.* **1986**, *30*, 73.
(55) Pellin, M. J.; Young, C. E.; Callaway, W. F.; Gruen, D. M. *Surf. Sci.* **1984**, *144*, 619.
(56) Kimock, F. M.; Baxter, J. P.; Pappas, D. L.; Kobrin, P. H.; Winograd, N. *Anal. Chem.* **1984**, *56*, 2782.
(57) See, for example: Kisker, E.; Schröder, K.; Campagna, M.; Gudat, W. *Phys. Rev. Lett.* **1984**, *52*, 2285. Gidley, D. W.; Köymen, A. R.; Capehart, T. W. *Phys. Rev. Lett.* **1982**, *49*, 1779.
(58) Gerstein, B. C.; Dybowski, C. R. *Transient Techniques in NMR of Solids*; Academic: New York, 1985.
(59) Zilm, K., private communication, 1987.
(60) See, for example: Onellion, M.; Hart, M. W.; Dunning, F. B.; Walters, G. K. *Phys. Rev. Lett.* **1984**, *52*, 380–383 and references therein.
(61) Posternak, M.; Krakauer, H.; Freeman, A. J.; Koelling, D. D. *Phys. Rev. B* **1980**, *21*, 5601.
(62) Posternak, M.; Baldereschi, A.; Freeman, A. J.; Wimmer, E. *Phys. Rev. Lett.* **1984**, *52*, 863.
(63) Koch, E.; Lang, N. D. *Phys. Rev. B* **1986**, *33*, 6567.
(64) Ruette, F.; Blyholder, G.; Head, J. D. *Surf. Sci.* **1984**, *137*, 491–505.
(65) Nordlander, P.; Tully, J. C., submitted to *Phys. Rev. Lett.*
(66) For a representative survey of applications of polarized radionuclides in condensed-matter physics and chemistry, see: Christiansen, J., Ed. *Hyperfine Interactions of Radioactive Nuclei*; Springer: Heidelberg, 1983. See also ref 67.
(67) See, for example, the studies of muon spin rotation experiments reported in the Proceedings of the VIIth International Conference on Hyperfine Interactions, Bangalore, India, 1986, as reported in *Hyperfine Interact.* **1987**, *35*.